

# Modelling GNSS-observed seasonal velocity changes of the Ross Ice Shelf, Antarctica, using the Ice-sheet and Sea-level System Model (ISSM)

Francesca Baldacchino<sup>1,2</sup>, Nicholas R. Golledge<sup>1</sup>, Mathieu Morlighem<sup>3</sup>, Huw Horgan<sup>1,4,5</sup>, Alanna V. Alevropoulos-Borrill<sup>1</sup>, Alena Malyarenko<sup>6,1</sup>, Alexandra Gossart<sup>1</sup>, Daniel P. Lowry<sup>7</sup>, and Laurine van Haastrecht<sup>1</sup>

<sup>1</sup>Te Puna Pātiotio | Antarctic Research Centre, Te Herenga-Waka, Victoria University of Wellington, Aotearoa | New Zealand

<sup>2</sup>Institute of Geodesy, Working Group Remote Sensing and Photogrammetry, Graz University of Technology, Austria

<sup>3</sup>Department of Earth Sciences, Dartmouth College, Hanover, NH 03755, USA

<sup>4</sup>Laboratory of Hydraulics, Hydrology and Glaciology (VAW), ETH Zurich, Zurich, Switzerland

<sup>5</sup>Swiss Federal Institute for Forest, Snow and Landscape Research (WSL), Birmensdorf, Switzerland

<sup>6</sup>School of Earth and Environment | Te Kura Aronukurangi, University of Canterbury | Te Whare Wānanga o Waitaha, Ōtautahi | Christchurch

<sup>7</sup>Department of Surface Geosciences, GNS Science, Lower Hutt, New Zealand

**Correspondence:** Francesca Baldacchino (francesca.baldacchino@tugraz.at)

**Abstract.** ~~Recent observations show that the ice flow of the Ross Ice Shelf (RIS) has a clear seasonal signal. The flow speed of floating ice shelves around the Antarctic ice sheet exhibit clear intra-annual variability. The drivers of these seasonal fluctuations in ice speed are still this variability however, remain~~ poorly understood. ~~We present here~~ Here, we present three new velocity datasets from GNSS stations on the ~~RIS~~ Ross Ice Shelf collected between early 2020 and late 2021. ~~It has previously been suggested that changes in sea surface height (SSH) was the main driver of these variations, requiring the grounding lines to migrate significantly further upstream than the point of hydrostatic equilibrium. Our new dataset, however, displays clear intra-annual velocity variability at the three sites, with 2021 and show that they have~~ two distinct peaks observed in austral summer and austral winter, ~~which is not~~. These measurements do not appear to be consistent with the yearly cycle of ~~SSH. Here~~, sea surface height, which has previously been identified as a possible driver. Here we investigate the potential role of basal ~~melting, and whether it would be capable of causing the observed variability in ice speed. In order to determine melt variability and use the Ross Ice Shelf as a testbed. First we identify the regions~~ where changes in melt would have the largest influence on ice ~~velocity, we use the automatic differentiation tool in the Ice-sheet and Sea-level System Model (ISSM) to identify the areas where the ice flow speed recorded at the GNSS sites are most sensitive to changes in basal melting. Next, we seasonally perturb Massachusetts Institute of Technology general circulation (MITgcm) basal melt rates in ISSM at~~ these identified sensitive regions until we reproduce similar velocity variability to the GNSS ice flow observations. Using this approach, we can reproduce the intra-annual velocity variation for GNSS sites near the calving front but only when high melt rates are applied. However, this approach fails for GNSS sites located far from the calving front and we speed at our GNSS sites using Automatic Differentiation. We then apply idealized sinusoidal perturbations to modeled basal melt rates at these specific locations to identify what magnitude of variability is needed to match the GNSS observed changes in ice speed. We show that,

20 while very local perturbations in basal melt can have a significant impact on ice flow speed, the perturbations required to match observations are significantly higher than expected, which may indicate that these perturbations are not realistic. We suggest that a combination of external forcings and internal mechanics may be needed to reproduce the observed intra-annual velocity variation at these sites. ~~While this study does not bring a definitive answer to the question of what the drivers of seasonality in ice flow are, this study shows that seasonal basal melt rates could explain the GNSS velocity variability on an annual timescale for two of the four GNSS sites. Additionally, our sensitivity maps highlight regions of the ice shelf where changes in basal melt most influence velocities and are a valuable addition to fieldwork campaigns and modelling studies. all the GNSS sites.~~

## 1 Introduction

The Antarctic Ice Sheet (AIS) contains the vast majority of Earth's freshwater and has the potential to raise global sea levels by 58 m (Mottram et al., 2019; Schlegel et al., 2018; Dirscherl et al., 2020). Over recent decades, the AIS has been losing mass at an accelerating rate due to the warming of the atmosphere and ocean (Pattyn et al., 2018; Shepherd et al., 2012, 2018; Jenkins et al., 2018; Rignot et al., 2019; Lipscomb et al., 2021). Ocean-forced basal melting and calving drive the largest mass losses on the AIS (Pattyn et al., 2018; Rignot et al., 2019; Adusumilli et al., 2020; Joughin et al., 2014). Floating ice shelves, in particular, provide buttressing to grounded ice and thus are vital for controlling AIS mass loss (Schoof, 2007; Gudmundsson, 2013; Dinniman et al., 2016; Joughin et al., 2013; Pattyn and Durand, 2013). ~~Ocean-forced basal melting thins ice shelves, reducing their buttressing ability of the grounded ice, which in turn increases ice discharge.~~ Recent observations have shown that some of these ice shelves show clear intra-annual variability in ice flow (e.g., Gwyther et al., 2018; Greene et al., 2018; Holland et al., 2019; Jenkins et al., 2018). While this flow variability is generally attributed to variability in external environmental forcings, the exact mechanism responsible for speed changes remains unclear. Gwyther et al. (2018), for example, found that there was high interannual variability in the Totten Ice Shelf surface elevation, velocity and grounding line retreat. ~~location due to variability in basal melting.~~ Greene et al. (2018) found that seasonal velocity variations observed at Totten Ice Shelf are due to seasonal variations in landfast sea ice concentrations at the calving front. More recently, Mosbeux et al. (2023) attributed the variability in flow speed of the Ross ice shelf to seasonal changes in Sea Surface Height (SSH).

The ~~Here, we focus on the~~ Ross Ice Shelf (RIS), which is Antarctica's largest ice shelf by area, and is approximately in balance (Moholdt et al., 2014; Rignot et al., 2013; Depoorter et al., 2013). ~~Currently, there is limited understanding of the influence of seasonal oceanic and atmospheric variability on the flow dynamics of the RIS. It is important to understand the impact of this seasonality on ice shelf flow as this may provide further understanding of the processes controlling ice shelf mass balance over longer timescales. Ice shelves flow by gravity-driven horizontal spreading with resistance to flow provided by shear at bay walls and pinning points. Changes in ice shelf dynamics, geometry, and mass can lead to changes in velocity on floating and grounded ice.~~ The RIS has typical flow speeds of several hundred meters per year, with the active Siple Coast Ice Streams and Byrd Glacier displaying velocities of > 300 m/a (Figure 1). ~~The ice shelf front exhibits the fastest flow rates of 800–1200 m/a (Figure 1). The Siple Coast Ice Streams and Transantarctic Mountain outlet glaciers are the main conduits~~

of ice discharging into the RIS from the West Antarctic Ice Sheet (WAIS) and East Antarctic Ice Sheet (EAIS), respectively (Figure 1).

55 Global Navigation Satellite System (GNSS) receivers can record near-continuously at high temporal resolution throughout the year and thus have the ability to measure seasonal variations in ice velocities (Brunt, 2008; King et al., 2011; Brunt and Macayeal, 2014). Typically, GNSS receivers are employed to measure ice velocities over 1–3 months in the austral summer and to highlight short timescale processes such as tidal variability (e.g. Bindschadler et al., 2003). In this study, we present  
60 new sites: the shear margin (Site 1) and the calving front (~~Site 2~~) near the Ross Island pinning point (Site 2), and the KIS grounding zone (Site 4; Figure 1). Additionally, the GNSS dataset previously reported in Mosbeux et al. (2023); Klein et al. (2020) (referred to as DR10 in previous studies and Site 3 here) are explored in this study.

Previous multi-season GNSS observations on the RIS have noted intra-annual (monthly to seasonal) velocity variations, with one distinct peak per year in the austral winter (Klein et al., 2020; Mosbeux et al., 2023). Two mechanisms have been  
65 proposed to explain this intra-annual variability. ~~Firstly~~First, Klein et al. (2020) investigated the impact of a seasonal cycle of spatially varying basal melt rates on the RIS using ice sheet modelling. Klein et al. (2020) used monthly basal melt rates from the ocean model described by Tinto et al. (2019). This ocean model was developed using a repeated annual cycle of forcing for the period 2001-2002 and therefore does not account for known inter-annual variability in atmospheric, oceanic and sea-ice conditions in the Ross Sea (Klein et al., 2020). They found that their modelled seasonal flow variations from basal melting were  
70 much smaller than the GNSS-observed (Klein et al., 2020). Therefore, Klein et al. (2020) concluded that the GNSS-observed intra-annual velocity variations on the RIS are most likely not driven by seasonal basal melt rates and that some other seasonal forcing must be dominant. ~~They found that their modelled variability of ice velocity was much smaller than their GNSS observations.~~ ~~More recently~~, Mosbeux et al. (2023) used ice sheet modelling to investigate whether the seasonal variability of ~~sea surface height (SSH) modifies~~ SSH would modify ice velocity through a combination of sea surface tilt and changing  
75 basal stresses at the grounding zone. Mosbeux et al. (2023) successfully reproduced the GNSS-observed intra-annual velocity variability at their GNSS sites if a sufficiently large cycle of SSH-induced basal shear stress change near the grounding line was parameterized in their ice sheet model. They found that, in order to capture the observed change in flow speed, they had to allow for the model grounding line to retreat significantly further upstream than what hydrostatic equilibrium would dictate, using a parameterization of viscoelastic processes (Mosbeux et al., 2023). ~~Furthermore~~More importantly, Mosbeux et al. (2023)  
80 modelled SSH forced velocity variability displays one distinct peak per year, in contrast to our GNSS observations, which all display two distinct peaks per year. This suggests that seasonal variability in SSH ~~is unlikely to~~ may not be the only forcing that explains the observed variability in velocities at our GNSS sites. ~~We therefore~~ To address this question, we turn again to the potential role of basal melt variability as it is known to be an important control on ice shelf dynamics.

The RIS basal melt rates are relatively low due to the cold dense water masses formed on the continental shelf blocking  
85 the sub-ice-shelf ocean cavity from warm Circumpolar Deep Water (CDW) intrusions (Moholdt et al., 2014; Stevens et al., 2020; Adusumilli et al., 2020). However, basal melt rates of the RIS vary spatially as they are driven by subsurface inflows of cold High Salinity Shelf Water (HSSW) that reach the grounding zone and seasonal inflows of summer-warmed Antarctic

Surface Water (AASW) at the calving front (Stewart et al., 2019; Stevens et al., 2020; Klein et al., 2020; Jendersie et al., 2018; Dinniman et al., 2016; Adusumilli et al., 2020). Recently, high basal melt rates have been observed at the calving front near  
90 Ross Island due to the seasonal inflow of summer-warmed AASW from the adjacent Ross Sea Polynya downwelling into the ice shelf cavity (Stewart et al., 2019; Malyarenko et al., 2019). Previous studies have suggested that RIS velocities may be modulated at seasonal to intra-annual timescales by basal melting at the calving front (Stewart et al., 2019; Tinto et al., 2019). ~~Ross Island has been identified as a sensitive region where changes in ice thickness can drive changes in ice shelf dynamics and mass balance. With predicted surface warming and declines in summer sea ice, these high basal melt rates along the calving front are projected to increase. Additionally, high basal melt rates may occur in the future due to changes in the primary modes of basal melting of the RIS. Such changes include increases in the amount of Modified Circumpolar Deep Water (mCDW) heat flux flowing onto the continental shelf and reducing the rate of sea ice formation. mCDW is formed by CDW flowing onto the continental shelf of the Ross Sea and mixing with the AASW and HSSW.~~

~~In this study, we aim to investigate whether perturbations in basal melt rates can reproduce the observed intra-annual variations in ice velocities at four sites across the RIS. We concluded that basal melt is not driving the observed intra-annual velocity variability on the RIS, but 'basal melting can explain some of the observed seasonality in ice flow'. Therefore, we aim to further test this hypothesis by (1) presenting three new GNSS datasets which display two distinct velocity peaks per year (a different intra-annual velocity variability to those presented in ) and (2) using a novel approach of combining the Automatic Differentiation tool in ISSM and perturbed. Here, we first map the sensitivity of ice flow speed at all available GNSS sites to basal melting to identify the regions of the RIS that are most sensitive to changes in basal melt. We then apply idealized sinusoidal perturbations to weekly MITgcm basal melt rates to enable us to identify whether seasonal changes in basal melt rates at identified sensitive regions can reproduce the observed identify what magnitude of variability is needed to match the GNSS observed changes in ice speed. We conclude by discussing how realistic these perturbations are, and whether basal melt variability could be the driver of the observed intra-annual velocity variability changes in flow speed. showed that RIS mass balance is sensitive to changes in basal melt at specific locations. Here we apply a similar approach to identify the regions where flow speed at GNSS locations is most sensitive to melt. We use multiple basal melt peaks as the basis for our phasing of the basal melt forcing, and apply perturbations on this forcing until we reproduce a similar velocity variability to the GNSS observations. Therefore, our study serves as a proof of concept, motivated by 'other as-yet-identified seasonal processes' driving the observed velocity variations on the RIS.~~

## 115 2 Locations and Methods

### 2.1 Global Navigation Satellite Systems locations

We first present results from three new GNSS sites (Sites 1, 2 and 4), and a previously reported GNSS site (Site 3) (Mosbeux et al., 2023; Klein et al., 2020) on the Ross Ice Shelf (Figure 1). The three new GNSS units were installed during field season the 2019/2020 austral summer and the data was/were downloaded in December 2021 (Sites 1, 2, and 4 in Figure 1). ~~These~~ The geodetic-grade GNSS units were battery-powered and deployed year round on the RIS ~~for multiple field seasons~~ to provide a  
120

long-term continuous ~~dataset that can observe observations of~~ intra-annual velocity ~~variations. The GNSS unit at variability.~~ GNSS observations from Site 3 is the same as that in were previously reported by Klein et al. (2020). Site 3 recorded between November 2015 and December 2016 and is described in more detail in ~~their study~~ (Klein et al. (2020) where it is referred to as DR10) (Figure 1).

125 Site 1 is located close to Ross Island, which is a major pinning point making it a sensitive region where changes in ice thickness are expected to influence the flow speed of the entire ice shelf (Gudmundsson et al., 2019; Fürst et al., 2016; Baldacchino et al., 2022; Reese et al., 2018) (Figure 1). Pinning points such as Ross Island provide resistance to ice shelf flow by modifying the balance of forces within the floating ice (Still et al., 2019; Cuffey and Paterson, 2010). This modification of forces has an effect everywhere on the ice shelf due to the balance of forces in floating ice being non-local (Still et al., 2019; Cuffey  
130 and Paterson, 2010). High basal melt rates with a seasonal signal have been observed close to the Ross Island pinning point (Stewart et al., 2019). Site 1 GNSS unit recorded every 30 seconds for 1 hour every 6 hours and has 80 days of data missing in July - October 2020, and 70 days in July - September 2021.

Site 2 is located ~~at~~ close to the ice front approximately ~~50 km~~ 50km from Ross Island and is likely expected to be influenced by seasonal changes in basal melting (Figure 1). High basal melt rates have been observed in this region and correlate with  
135 declines in sea ice cover and warming of the AASW during the austral summer (Stewart et al., 2019). Site 2 is located within the "passive" region of the ice shelf and thus this region can be removed without ~~impacting the mass balance reducing the buttressing potential~~ of the ice shelf (Fürst et al., 2016). Site 2 GNSS unit recorded every 30 seconds ~~over 24 hours~~ and has 104 days of data missing in June - November 2020 and 30 days in July - August 2021.

Site 3 is located in the mid-shelf region of the RIS (200km from the calving front) and is the same site (referred to as DR10)  
140 previously reported in Klein et al. (2020) and Mosbeux et al. (2023) (Figure 1). Ice flow in the central portion of the RIS is primarily extensional which leads to along-flow thinning (Das et al., 2020). There are no pinning points or ice rises within ~~the vicinity~~ 300km of Site 3, and no observations of high basal (Adusumilli et al., 2020) or surface (Agosta et al., 2019) melt rates here. The Site 3 GNSS unit recorded every 30 seconds ~~over 24 hours~~ for 1 year (2015 - 2016), with a few days dropped in the austral winter of 2016 (Klein et al., 2020).

145 Finally, Site 4 is located at the Kamb Ice Stream (KIS) grounding line (Figure 1). The KIS has been inactive for the last 160 years likely due to a change in subglacial hydrology (Retzlaff and Bentley, 1993; Thomas et al., 2013; Hulbe et al., 2016). The KIS used to flow at speeds of 350 m/a but presently flows at speeds of less than 5 m/a (Rignot et al., 2017; Ng and Conway, 2004). Studies have indicated that the KIS could reactivate this century due to its hydrological setting and the length of time it has been inactive (Bougamont et al., 2015; van der Wel et al., 2013). Site 4 GNSS unit recorded every 30 seconds and operated  
150 continuously, but was shifted approximately 2.7km upstream in December 2020.

## 2.2 Global Navigation Satellite Systems processing

GNSS data were processed using the Precise Point Positioning (PPP) methodology (Zumberge et al., 1997; Tétreault et al., 2005) and Natural Resources Canada's Canadian Spatial Reference System Precise Point Positioning (CSRS-PPP) post-

processing service<sup>1</sup>. For the 30-second sampled continuous data (Sites 2, 3, and 4), data were divided into 3-hour segments  
155 and processed statically to obtain a single position every 3 hours. For Site 1, which has a different sampling frequency, the data  
were divided into 1-hour segments every 6 hours and a single position was obtained every 6 hours. Data processing was iterated  
whereby the initial positions were updated with the first processing results and then reprocessed to obtain new position solu-  
tions. The position solutions were then projected into polarstereographic coordinates (EPSG:3031) and then used to estimate  
site velocity by weighted linear regression through x and y coordinates. The position weightings were provided by the reported  
160 processing uncertainty. Regression gradients provided velocities in the x and y direction ( $v_x, v_y$ ) with gradient uncertainties  
propagated to provide uncertainties in velocity and direction. The linear regression of positions was estimated at every time  
step (either 3 hourly or 6 hourly) over centered time windows of 8 weeks duration. This provides a low-noise time series with  
a high temporal fidelity (albeit smoothed) that shows the seasonal cycle in velocity without aliasing spring-neap tidal velocity  
signals. The use of the 8-week duration to estimate velocity means that otherwise rapid changes in velocity are smoothed over  
165 an 8-week period. Other time window lengths were tested and the seasonal signal was ~~seen~~found to be largely independent of  
the length used. The resulting uncertainties ~~were~~are low with 99% of the  $1\sigma$  velocity uncertainties less than 0.04 m/a for ~~sites~~  
Sites 1 and 3, less than 0.06 m/a for Site 2, and less than 0.01 m/a for Site 4. We present all velocities as both absolute velocity  
(Figure 2) and as the deviation from the initial velocity to facilitate comparison with the modelling results (Figure 4). We also  
present detrended position and direction results for each site (Figures A1–A4).

## 170 2.3 Automatic Differentiation

We ~~used~~use Automatic Differentiation (AD, Sagebaum et al., 2019) in the Ice-sheet and Sea-level System Model (ISSM) to  
explore the influence that changes in basal melt have on the ice velocity at each GNSS site. The complete model description is  
available in Baldacchino et al. (2022). Here, instead of computing the sensitivity of the model’s final volume above flotation,  
we ~~were~~are interested in the sensitivity of the model velocity at these four GNSS sites. AD ~~allowed~~allows us to efficiently  
175 map by how much the velocity at each site would be affected if we ~~perturbed~~perturb the ocean-induced melt at the scale of the  
model mesh.

The model domain ~~covered~~covers the entire RIS and has a non-uniform mesh with a resolution of ~~1 km~~1 km at the grounding  
lines and in the shear margins, ~~20 km~~20 km in the ice sheet interior, and at most ~~10 km~~10 km within the ice shelf. The basal  
friction coefficient over grounded ice and the ice viscosity parameter of the floating ice,  $B$ , ~~was~~is inferred through a data  
180 assimilation technique (Morlighem et al., 2010, 2013) to reproduce observed InSAR surface velocities from the MEaSURES  
data-set (Rignot et al., 2017; Baldacchino et al., 2022). Environmental boundary conditions ~~included~~include RACMO2.3p2  
Surface Mass Balance (Van Wessem et al., 2018) and Massachusetts Institute of Technology general circulation (MITgcm)  
basal melt rates (Losch, 2008; Holland and Jenkins, 1999; Davis and Nicholls, 2019; Baldacchino et al., 2022). The ice sheet  
model ~~was~~is run forward for 20 years to allow the grounding line position and ice geometry to relax.

185 After relaxation, we ~~ran~~run the AD model for 6 months and ~~evaluated~~evaluate the sensitivity of the final velocity at each of  
the four GNSS sites to perturbations in basal melting rates under floating ice,  $\dot{M}_b$ . Automatic differentiation ~~provided~~provides

---

<sup>1</sup><https://webapp.csrscs.nrcan-rncan.gc.ca/geod/tools-outils>. Last accessed: 15.08.2023

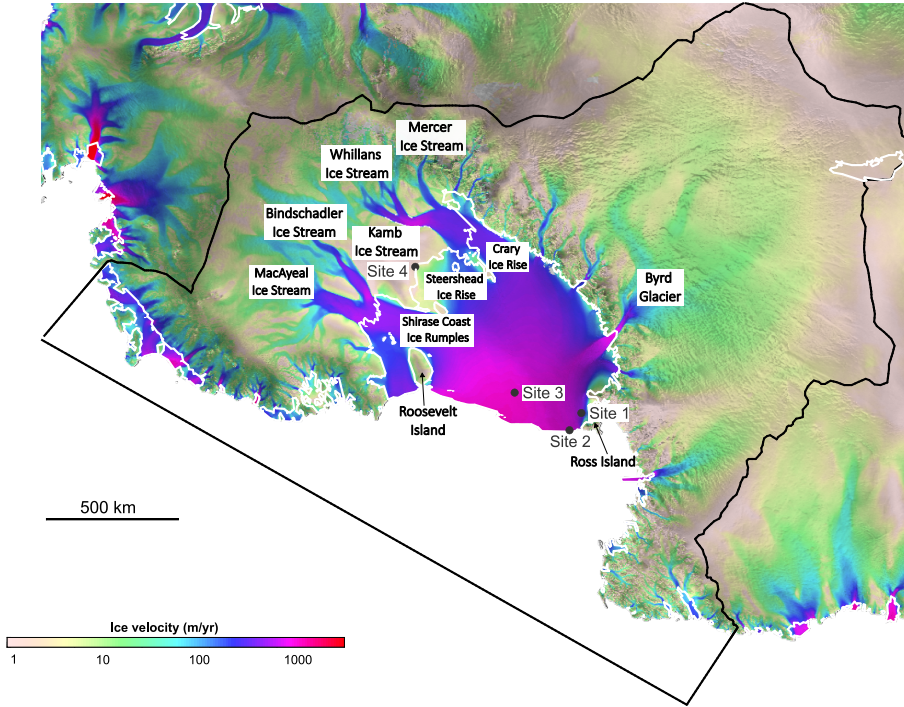


**Figure 1.** GNSS station locations overlain on modelled Ross Ice Shelf surface velocities. The grounding line is marked in white. GNSS sites shown are: Site 1 (shear margin region), Site 2 (calving front), Site 3 (mid-shelf region), and Site 4 (KIS grounding zone). Other locations discussed in this study are also labelled. These include the Siple Coast Ice Streams: Mercer Ice Stream (MIS), Whillans Ice Stream (WIS), Kamb Ice Stream (KIS), Bindschadler Ice Stream (BIS), and MacAyeal Ice Stream (MacIS). Byrd Glacier (BG) and Ross Island are also labelled. In addition, the ice rises are labelled on the Siple Coast: Crary Ice Rise (CIR), Steershead Ice Rise (SIR), Shirase Coast Ice Rumples (SCIR), and Roosevelt Island. The projection of this map and all others presented is polar stereographic with a true scale at  $-71^\circ$  (EPSG:3031).

the gradient of the final velocity at each site,  $v_i$ , to basal melt:  $\mathcal{D}v_i(\dot{M}_b)$ . In other words, the first order response of the velocity to a given perturbation  $\epsilon\delta\dot{M}_b$  in  $\dot{M}_b$  (where  $\epsilon \in \mathbb{R}$ , and  $\delta\dot{M}_b$  was-is defined over the entire model domain  $\Omega$  that can be spatially variable) was-is given by:

$$190 \quad v_i(\dot{M}_b + \epsilon\delta\dot{M}_b) = v_i(\dot{M}_b) + \epsilon \int_{\Omega} \mathcal{D}v_i(\dot{M}_b) \delta\dot{M}_b d\Omega + \mathcal{O}(\epsilon^2). \quad (1)$$

The gradient,  $\mathcal{D}v_i(\dot{M}_b)$  (in  $\text{m}^{-2}$ ), therefore highlighted-highlights the regions where the modelled velocity at a given site was-is most sensitive to changes in  $\dot{M}_b$ , and the regions where changes in  $\dot{M}_b$  would not affect the final velocity at a first order.

This approach ~~provided~~ provides four sensitivity maps, one for each site. Figure A5 shows the areas where this sensitivity ~~was is~~ higher than our threshold value of  $2e-11 \text{ m}^{-2}$ . The sensitivity threshold value of  $2e-11 \text{ m}^{-2}$  ~~was is~~ chosen to highlight the areas sensitive to basal melt changes. Choosing a lower sensitivity threshold would enlarge the surface area over which the perturbation would need to be applied, and a higher sensitivity threshold would have the opposite effect. We chose a sensitivity value of  $2e-11 \text{ m}^{-2}$  to highlight areas of high sensitivity over a surface area that is not too restrictive or extensive across the ice shelf (Figure A5). We also ~~included~~ include a lower sensitivity value of  $0.5e-11 \text{ m}^{-2}$  (Figure A6) in our experiments to highlight that the modelled velocity variations are similar for both sensitivity thresholds. These sensitive regions, highlighted in dark red, show where an increase in basal melt rates leads to an increase in ice velocity for each site, and therefore where changes in melt rates would impact ice velocity at these sites the most. ~~Sensitive regions are sometimes hundreds of kilometres from the GNSS stations.~~ Finally, we ~~performed~~ perform additional experiments where we only ~~perturbed~~ perturb the basal melt rates at the identified sensitive regions ~~along the calving front~~ close to the Ross Island pinning point (Figure A7). These experiments ~~were are~~ performed to understand whether ~~seasonal~~ changes in basal melting ~~along at~~ the calving front can solely reproduce the ~~seasonal~~ intra-annual velocity variations observed at the GNSS sites.

## 2.4 Modelled perturbed basal melt

~~A~~ ~~We next perform a~~ set of modelling experiments within ISSM ~~was then performed, where to identify what magnitude of basal melt variability is needed to match the GNSS observed changes in ice speed. In these modelling experiments,~~ the MITgcm baseline basal melt rates ~~were are~~ perturbed seasonally (using a sine function that includes both melting and refreezing) (Figures A8 and A9) at regions identified as highly sensitive in the final AD map for each GNSS ~~site:~~ sites:

$$\dot{M}_b(t) = \begin{cases} \text{MITgcm}(t) + p \sin(4\pi \times t + \pi), & \text{if one or more maps shows a sensitivity } > 2e-11 \text{ m}^{-2} \\ \text{MITgcm}(t), & \text{otherwise} \end{cases} \quad (2)$$

where  $\text{MITgcm}(t)$  ~~was is~~ the unperturbed melt rate from the MITgcm (Figure A8), and  $p$  ~~was is~~ the amplitude of the perturbation, taken here as 0, 20, 40, 60 or 80 m/a. A sine function with two peaks ~~was is~~ used to simulate two basal melt peaks per year (Figure A9). These peaks ~~were modelled happen~~ in April and October using the ~~+3 radiant in the sine function~~  $+\pi$  phase shift. Two basal melt peaks per year ~~were are~~ needed to reproduce the observed intra-annual velocities at the GNSS sites. The unperturbed MITgcm basal melt rates ~~displayed display~~ a seasonal signal with a clear peak in the austral summer, and multiple smaller peaks throughout the year, highlighting that the basal melt rates ~~have large already have large intra-annual variability~~ (Figure A8). However, the amplitude of this seasonal variability in the baseline MITgcm basal melt rates ~~was is~~ not large enough and the phasing incorrect to reproduce the GNSS observed velocity variability. The ~~MITgcm basal melt rates are imperfect and are unlikely to include all possible temporal and spatial variability in basal melt rates, especially at the grounding lines. Hence the need for perturbations in addition to the unperturbed MITgcm basal melt rates, as described in equation (2) (Figure A9). The model was model is~~ run forward for an additional 20 years to allow the geometry and grounding line to stabilize. ~~The model was then run forward 2 years~~ using the same model setup as described above (Section 2.3).



## 2.5 Modelled seasonal sea surface height

225 As discussed previously, Mosbeux et al. (2023) showed that variability in the RIS velocities ~~is driven by~~ can be attributed  
to seasonal variability in sea surface height (SSH). To explore this potential driver of velocity variability for our new GNSS  
datasets, we ~~forced~~ force our model with the SSH perturbations that Mosbeux et al. (2023) used in their study. Mosbeux  
et al. (2023) interpolated the SSH forcing from the ocean model of Tinto et al. (2019) as a monthly forcing and applied  
a parameterisation of the friction in the grounding zone (refer to Mosbeux et al. (2023) for further details). We ~~interpolated~~  
230 interpolate the SSH forcing onto our ISSM grid for the RIS, following the same model set-up described in Section 2.3. Mosbeux  
et al. (2023) highlights that there are two main effects of SSH variability on ice shelf velocities: (1) changes in driving stress  
and (2) changes in basal stress through grounding line migration. Our modelling experiments ~~are only based on the hydrostatic~~  
~~equilibrium of the grounding line~~ only accounts for hydrostatic-based grounding line migration and therefore do not account  
for the potential role of viscoelasticity (similar to modelling experiment  $\Delta$ LB2 in Mosbeux et al. (2023)).

## 235 3 Results

### 3.1 GNSS Velocities

#### 3.1.1 Site 1

GNSS velocity observations for Site 1 are presented in Figure 2. Site 1's velocities range from a maximum of 447 m/a to a  
minimum of 441 m/a with a clear decrease in velocities of 4 m/a over the two years (Figure 2). ~~The velocity variations are~~  
240 ~~small throughout the two years, however, an~~ Figure 2 displays an intra-annual ~~signal is observed at Site 1 (Figure 2).~~ Figure 2  
displays signal with two velocity peaks: one in June (austral winter) and one in January (austral summer). These velocity peaks  
are preceded by periods of acceleration (April - June and November - January) and periods of deceleration (February - April  
and July - October) (Figure 2). An acceleration of 2 m/a for the peak in June 2020, 1.5 m/a for the peak in January 2021 and  
1.5 m/a for the peak in June 2021 highlights the largest seasonal velocity variations at Site 1 (Figure 2).

#### 245 3.1.2 Site 2

GNSS velocity observations for Site 2 are presented in Figure 2. The velocities range from a maximum of 745 m/a to a  
minimum of 739 m/a, with a clear intra-annual signal observed at Site 2 (Figure 2). Two distinct velocity peaks are observed  
at Site 2: one in December (austral summer) and one in July (austral winter). These velocity peaks are preceded by periods of  
acceleration (April - July and October - December) and periods of deceleration (January - April and July - October) (Figure  
2). ~~Similar to Site 1, the velocity variations are small throughout the two years, however, a larger acceleration is observed in~~  
250 ~~the lead-up to the peaks compared to Site 1.~~ An acceleration of 5 m/a for the peak in July 2020, an apparent acceleration of 1.5  
m/a for the peak in December 2020 ~~, and~~ (the lower limit was not observed), and an acceleration of 3 m/a for the peak in July  
2021 highlights the largest seasonal velocity variations at Site 2 (Figure 2). Site 2 displays a larger maximum velocity of 745

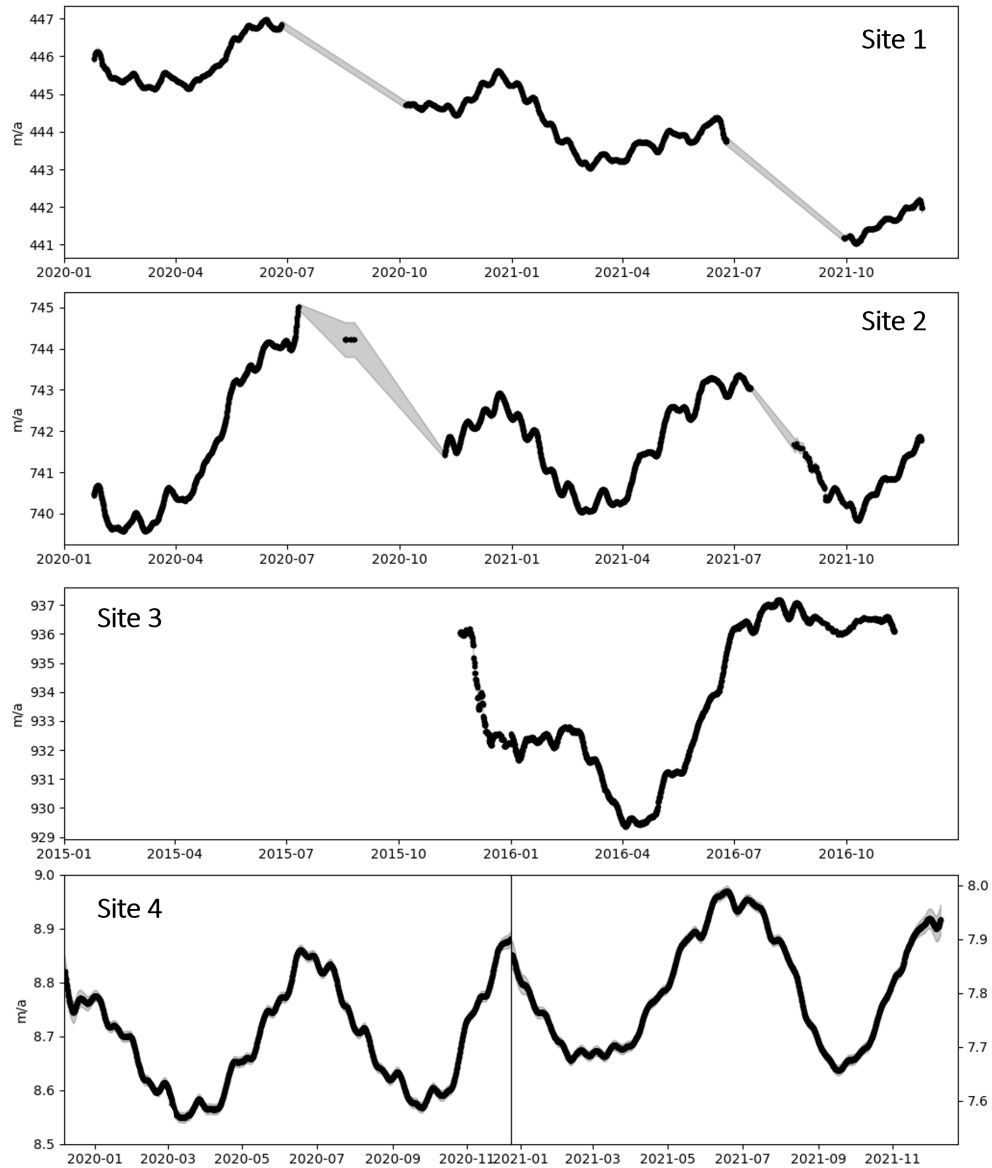


**Figure 2.** The GNSS velocities (in m/a) at Site 1 (shear margin region), Site 2 (calving front), Site 3 (mid-shelf region), and Site 4 (KIS grounding zone). The uncertainties are provided in the grey windows enclosing the black lines. These uncertainties are not visible in a few places, as they are very small. Detrended position and direction for each site is shown in Figures A1-A4

255 m/a compared to Site 1's maximum velocity of 447 m/a. Overall, the velocities neither decreased nor increased significantly throughout the two years at Site 2.

### 3.1.3 Site 3

GNSS velocity observations for Site 3 ~~are presented in Figure 2. The velocities~~ range from a maximum of 937 m/a to a minimum of 929 m/a and thus display higher maximum velocities compared to Sites 1 and ~~2-2 (Figure 2).~~ However, Site 3's intra-annual signal is different to Sites 1 and 2, with a small peak observed in March (austral summer) and a large peak in  
260 August (austral winter) (Figure 2). These velocity peaks are preceded by periods of acceleration (January - March and April - August) and periods of deceleration (March - April and September - December) (Figure 2). ~~Similar to Sites 1 and 2, the velocity variations throughout the year are small, however, Site 3 displays the largest acceleration in the lead-up to a peak.~~ A small acceleration of 1 m/a for the peak in March 2016 and a much larger acceleration of 8 m/a for the peak in August 2016 is observed (Figure 2). Site 3 was also presented in Klein et al. (2020); Mosbeux et al. (2023) (referred to as DR10), and they  
265 display similar results to ours. Both studies display a small velocity peak in January and a large velocity peak in July (Klein et al., 2020; Mosbeux et al., 2023). The velocity variability ranges from -6 m/a in March, and +6 m/a in July, which is a similar range of velocity values found in this study (-7 m/a in April to +1 m/a in August) (Figure 4). However, our velocity peaks ~~for Site 3~~ (March and August) are offset by 1-2 months compared to the findings presented in Klein et al. (2020); Mosbeux et al. (2023). These ~~small~~ differences in the phasing of the intra-annual velocity variability are likely due to small differences in  
270 methodology between the studies, such as the use of T-TIDE analysis (Pawlowicz et al., 2002) and the time window used for smoothing the datasets (~~used 1-month sliding window, used longer timescales by using a sliding Gaussian filter with a 2-week standard deviation, and we used a time window of 2 months~~).

### 3.1.4 Site 4

~~GNSS velocity observations for Site 4 are presented in Figure 2. Figure 2 shows that~~ The stagnation of KIS results in Site  
275 ~~4 has the smallest maximum velocities of 9.0 m/a compared to the other GNSS sites. The KIS has been inactive for the last 160 years and thus the velocities are very low at the grounding line compared to~~ 's low velocities compared to Sites 1, 2, and ~~3-3 (Figure 2).~~ Site 4 displays a clear intra-annual signal which is similar to Sites 1 and 2 (Figure 2). Two velocity peaks are observed at Site 4 for the years 2020 and 2021: one in December (austral summer) and one in June (austral winter) (Figure 2). Site 4 has the most complete record of GNSS velocity measurements for two years and thus highlights the intra-annual velocity  
280 variation nicely clearly. These velocity peaks are preceded by periods of acceleration (March - June and October - December) and periods of deceleration (January - March and July - August) (Figure 2). Site 4 displays ~~the smallest velocity variations compared to the other GNSS sites with an a small~~ acceleration of 0.4 m/a for the peak in June 2020, 0.3 m/a for the peak in December 2020, 0.3 m/a for the peak in July 2021 and 0.3 m/a for the peak in December 2021 (Figure 2). ~~also observed that the further the GNSS sites are~~ The magnitude of intra-annual variability at each site scales with distance from the calving front,  
285 ~~the smaller the intra-annual velocity variation~~ also observed by Klein et al. (2020).

A fortnightly signal is found in the displacement at all GNSS sites and we attribute this to the response of the ice shelf to spring-neap variability in the tidal cycle (Padman et al., 2003; Ray et al., 2021; Rosier and Gudmundsson, 2020). This

fortnightly tide-forced variability is dampened by our use of an 8-week window for our velocity estimates (Mosbeux et al., 2023).

## 290 3.2 Sensitivity Maps

The AD model produced sensitivity maps show that high sensitivity is observed at the pinning points and ice rises downstream of the Siple Coast ice streams (i.e., Roosevelt Island, Crary Ice Rise, Steershead Ice Rise, and the Shirase Coast Ice Rumples) for all GNSS sites (Figures 1 and 3). For ~~GNSS~~ Sites 1, 2, and 3 we also see high sensitivity to changes in basal melting at the calving front near the Ross Island pinning point. Changes in basal melting can result in detachment from pinning points and ice rises resulting in changes in ice speed (Still et al., 2019; Baldacchino et al., 2022; Reese et al., 2018). Ross Island is a structurally critical region and Gudmundsson et al. (2019) found that ~~rapid~~ melting there influences the flow speed of the entire RIS. Our sensitivity maps confirm this finding, highlighting that changes at and/or near the Ross Island pinning point influence velocities at Sites 1, 2, and 3. It is also important to highlight that Sites 1 and 2 are situated close to the Ross Island pinning point, and thus have high sensitivity to local changes in basal melt.

300 Additionally, high sensitivity is observed at the Siple Coast Ice Streams and Byrd Glacier grounding lines for Sites 2 and 3 (Figures 1 and 3). The grounding lines show high sensitivity because changes in basal melting there can lead to changes in basal friction and grounding line retreat (Baldacchino et al., 2022). These changes in basal friction can drive changes in the ice streams and outlet glaciers' flow dynamics and discharge (Baldacchino et al., 2022; Pattyn, 2017; Shepherd et al., 2018). We observe high sensitivity at the near-stagnant KIS grounding zone for Site 4, and no sensitivity elsewhere for this GNSS site. 305 This high sensitivity at the KIS grounding zone highlights that local changes in basal melt at the grounding zone can influence the velocities at Site 4 and changes in basal melt elsewhere on the ice shelf do not affect Site 4 velocities.

Finally, high sensitivity within the interior of the ice shelf and directly downstream of active ice streams and outlet glaciers is observed for GNSS Sites 2 and 3 (Figures 1 and 3). Sensitivity to changes in basal melting is also observed at the "passive" region (blue outline in Figure 3 identified by Fürst et al. (2016)) for ~~GNSS~~ Sites 2 and 3. This indicates that local changes in 310 basal melt affect the velocities at Sites 2 and 3 as both these sites are located in the "passive" region. Overall, the sensitivity maps show that GNSS Sites 2 and 3 velocities have high sensitivity to basal melting across the majority of the ice shelf, compared to Sites 1 and 4, which have higher sensitivities to local changes in basal melting.

## 3.3 Modelled Velocities

The modelled velocity variations are compared to the GNSS velocity variations (change from the initial velocity) for each site 315 in Figure 4. We model two distinct velocity peaks: one in January (austral summer) and one in June (austral winter) for the ~~basal melt perturbation experiments. We perturbed the basal melt rates seasonally~~ experiments using our idealized sinusoidal basal melt perturbation at the identified sensitive regions ~~to reproduce these two velocity peaks at all the GNSS sites. These sensitive regions are located at the calving front near the Ross Island shear zone for Sites 1, 2, and 3 and pinning points downstream of the Siple Coast Ice Streams and at their grounding lines for Sites 2, 3, and 4.~~ For all GNSS sites, we observe that the 320 intra-annual velocity variation is small when we perturb the basal melt rates by a magnitude of 20 m/a, and this intra-annual

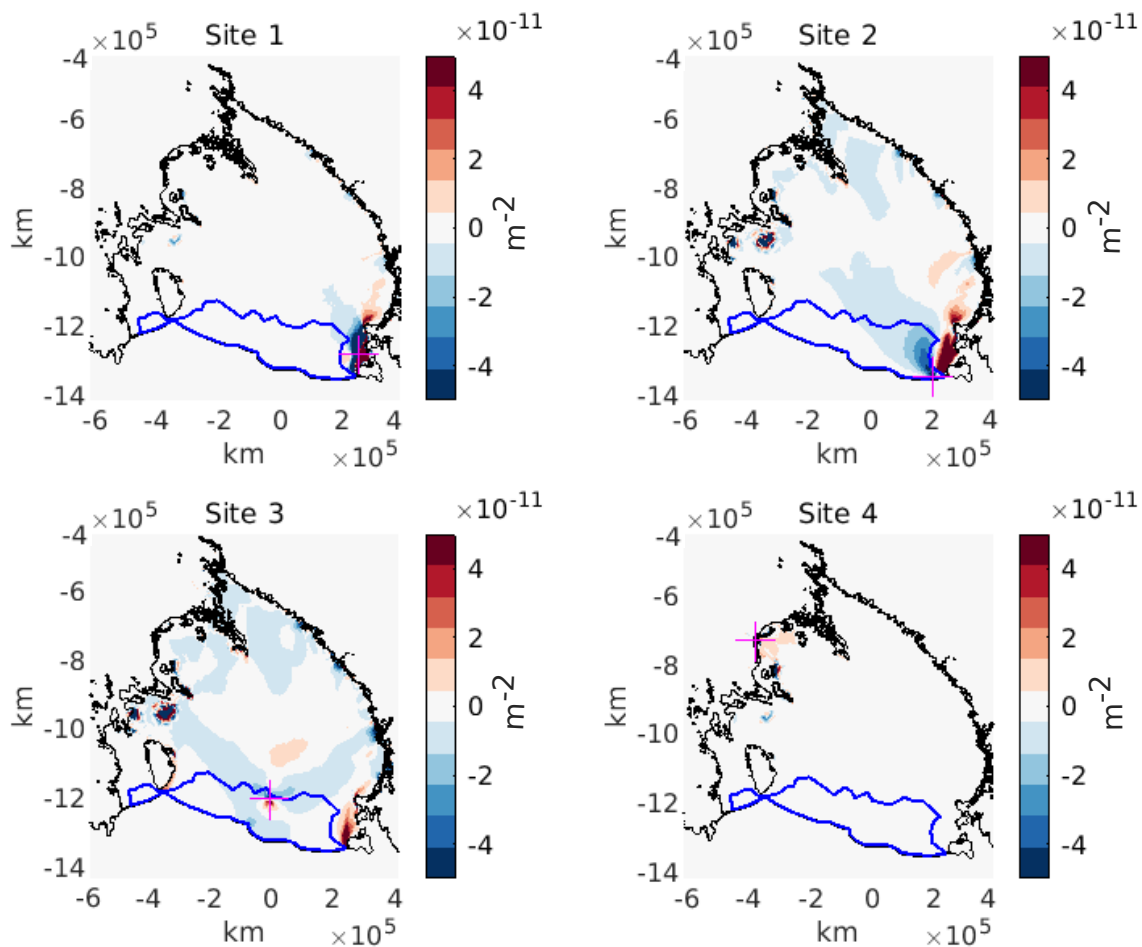


**Figure 3.** Sensitivity maps of the final velocity at each of the four GNSS sites to basal melt rates under floating ice  $\dot{M}_b$  over 40–20 years (in  $\text{m}^{-2}$ ). The sensitivity maps highlight that an increase (red) or decrease (blue) in basal melt rates at identified sensitive regions increases or decreases the velocities at the GNSS sites. The grounding line (black line) and passive ice (blue line) on the RIS identified by Fürst et al. (2016) are highlighted. The GNSS sites are identified using pink markers.

velocity variation quadruples when we perturb the basal melt rates by a magnitude of 80  $\text{m/a}$  (Figure 4). The dotted black line in Figure 4 highlights the experiments which used the lower sensitivity value of  $0.5\text{e-}11 \text{ m}^{-2}$  (Figure A6). Figure 4 shows that for GNSS-Sites 1, 2, and 3 the use of the lower sensitivity value threshold (dotted black line) did not significantly affect the final modelled velocity variations. However, for Site 4 the use of a lower sensitivity threshold increased the velocity peaks by about 20% due to more sensitive areas near the KIS grounding zone being perturbed. Additionally, the solid black line in Figure 4 highlights the experiments in which the basal melt was only perturbed at the calving front near Ross Island. Figure 4 Additionally, Figure 4 shows that for Sites 1, 2, and 3 the perturbation of basal melt rates close to Ross Island (solid

330 black line) produces similar velocity variations to the other model experiments. However, for Site 4 the velocity variations are much smaller due to being insensitive to the perturbed regions. The modelled absolute velocity values are similar to the GNSS absolute velocity values for Site 1 but are larger than the GNSS absolute velocity values for Sites 2, 3, and 4 (Figure A10). However, in this study, we focus on reproducing and analysing the GNSS velocity variations in our model simulations, even when large amplitudes are employed for the perturbation.

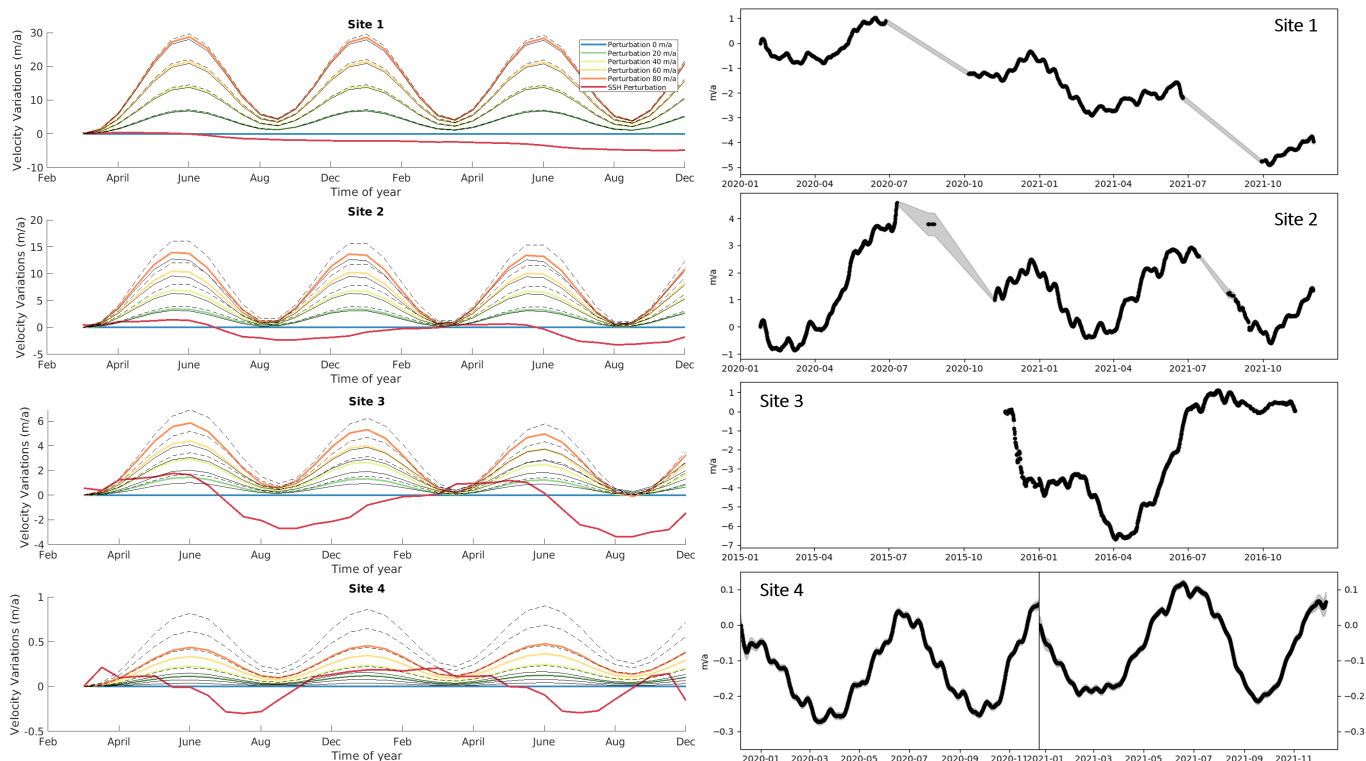


**Figure 4.** The modelled (left) and GNSS (right) velocity variations (in m/a) at each GNSS site: Site 1 (shear margin region), Site 2 (calving front), Site 3 (mid-shelf region), and Site 4 (KIS grounding zone). The dotted black line represents the additional sensitivity threshold value experiment (lower sensitivity value of  $0.5e-11 \text{ m}^{-2}$ ) and the solid black line represents the additional sensitivity experiment where we only perturbed the basal melt rates at the calving front close to Ross Island. Note here that we are comparing velocity changes induced by perturbed basal melt rates at identified sensitive regions to velocity changes induced by raw SSH over the entire domain.

335 Our basal melt perturbed model predicts-produces an intra-annual variation in velocity at Site 1 ranging from 1 m/a to 5 m/a for 20 m/a basal melt perturbation and 6 m/a to 28 m/a for the 80 m/a basal melt perturbation (Figure 4). An acceleration increase of 4 m/a for the velocity peaks in January and June is observed in the 20 m/a basal melt perturbed model experiments, which is most similar to Site 1's GNSS observed accelerations of 2 m/a for the velocity peak in June 2020, 1.5 m/a for the velocity peak in January 2020 and 1.5 m/a for the velocity peak in June 2021 (Figure 4). The seasonal SSH perturbed model

displays little to no intra-annual velocity variability for Site 1 (Figure 4). ~~However, the SSH forced velocities decrease over time similar to the GNSS observations (Figure 4).~~

340 The basal melt perturbed modelled intra-annual velocity variations at Site 2 range from 0 m/a to 3 m/a for 20 m/a basal melt perturbation and 2 m/a to 13 m/a for the 80 m/a basal melt perturbation (Figure 4). The phasing of the modelled velocity peaks (January and June) are offset by one month compared to the GNSS observed velocity peaks (December and July) ~~at Site 2~~ (Figure 4). However, the ~~peak in velocity occurs at the end of December, and the beginning of July which is similar to our modelled velocity peaks in January and June.~~ The 20 m/a basal melt perturbed modelled velocity variation is similar in  
345 amplitude to the GNSS velocity variations. An ~~acceleration~~ increase of 3 m/a for the peaks in January and June is observed in the 20 m/a basal melt perturbed model experiments, which is most similar to Site 2's GNSS observed accelerations of 5 m/a for the peak in July 2020, 1.5 m/a for the peak in December 2020 and 3 m/a for the peak in July 2021 (Figure 4). The seasonal SSH perturbed model displays an intra-annual velocity variability with a different phasing ~~and but similar~~ amplitude to the GNSS observations at Site 2 (Figure 4). The SSH forced velocities display one distinct peak per year (late May), with a  
350 velocity minimum ~~displayed~~ in August (Figure 4).

For Site 3, the modelled intra-annual velocity variations range from 0 m/a to 1 m/a for 20 m/a basal melt perturbation and 1.5 m/a to 4 m/a for the 80 m/a basal melt perturbation (Figure 4). The phasing of the modelled velocity peaks ~~occur in~~ (January and June, ~~which is different from~~) is offset by a couple of months compared to the GNSS observed velocity peaks ~~in~~ (March and August ~~for Site 3~~) (Figure 4). ~~Therefore, the phasing of the modelled velocity variations is offset by a couple of months.~~  
355 ~~Additionally, the amplitude of the modelled velocity peaks is smaller compared to the GNSS observed velocity peaks at Site 3. An acceleration of~~ Additionally, an increase of 1 m/a for the peak in March and 8 m/a for the peak in August is observed by the GNSS receiver at Site 3 (Figure 4). None of the basal melt perturbed modelled velocity variations capture an acceleration of 8 m/a in August (Figure 4). ~~Overall, the amplitude of the modelled velocity variation is significantly smaller compared to the GNSS measurements at Site 3. We display~~ We model two velocity peaks, whereas Klein et al. (2020) ~~displayed modelled~~  
360 one velocity peak in late May, with a smaller velocity range (-0.18 to +0.18 m/a). ~~This is likely due to the type of perturbations (i.e., magnitude and phasing) used in this study.~~ Furthermore, the seasonal SSH perturbed model displays an intra-annual velocity variability with a different phasing to the GNSS observations (Figure 4), but the amplitude of velocity variations is most similar to the observations. The SSH forced velocities display ~~one peak per year, similar to Site 2, in late May, with a velocity maximum in May and~~ a velocity minimum ~~displayed~~ in August. ~~However, Site 3 displays one distinct peak per year similar to the SSH forced velocity variability, and there is a closer similarity in the amplitude of velocity variations between the SSH forced velocities and the GNSS observations (Figure 4).~~ Mosbeux et al. (2023) modelled a velocity peak in August for Site 3, highlighting that our modelled velocity peak is offset by a couple of months. This may be due to our modelling experiments not taking into account the potential role of viscoelasticity.

Finally, ~~we model the lowest intra-annual velocity variation at Site 4 when perturbing the basal melt rates, which is similar to the GNSS measurements (Figure 4).~~ ~~The~~ the modelled intra-annual velocity variations at Site 4 range from 0.01 m/a to 0.04 m/a for 20 m/a basal melt perturbation and 0.04 m/a to 0.15 m/a for the 80 m/a basal melt perturbation (Figure 4). The phasing of the modelled velocity variations is similar to the GNSS-measured velocity variations with a clear intra-annual signal observed ~~at~~

~~Site 4.~~ The modelled velocity peaks occur in January and June which is similar to the GNSS-measured velocity peaks at the end of December and in June (Figure 4). However, none of the modelled velocity variations of the basal melt perturbation experiments could reproduce the amplitudes of the GNSS observed velocity variations. An ~~acceleration-increase~~ of 0.4 m/a for the peak in June 2020, 0.3 m/a for the peak in December 2020, 0.3 m/a for the peak in July 2021 and 0.3 m/a for the peak in December 2021 (Figure 4). An ~~acceleration-increase~~ of 0.11 m/a for the peaks in January and June is observed in the 80 m/a basal melt perturbed model experiments and is most similar to the GNSS-measured velocity variations at Site 4. ~~Similarly, to Site 3, overall the amplitude of the modelled velocity variation is significantly smaller compared to the GNSS measurements at Site 4.~~ The seasonal SSH perturbed model displays an intra-annual velocity variability with only one velocity peak per year (February) (Figure 4). ~~This phasing is different from our GNSS observations which display two distinct velocity peaks per year (December and June). However,~~ but the amplitude of velocity variations is most similar to the GNSS observations, ranging from -0.4 to 0.3 m/a (Figure 4).

~~For all GNSS sites, an increase in basal melt rates accelerates the velocities compared to the control run (Figure 4). We would expect this as the seasonally elevated melt rates lead to short-term thinning and acceleration of the ice shelf. The amplitude of modelled velocity variability decreases with increasing distance from the calving front, with the largest velocity variations modelled at Sites 1 and 2, and the smallest at Site 4. However, the GNSS units record the largest amplitude in velocity variation at Site 3 which also agrees with and~~

## 4 Discussion

### 390 4.1 Intra-annual velocity variability

~~The model captures a seasonal signal in velocity that is similar in phasing and magnitude to the GNSS observations at Sites 1 and 2 when~~

#### 4.1 Local perturbations

In this study, instead of perturbing basal melt rates (with a magnitude of 20 m/a) at sensitive regions. However, for Site 3, the magnitude of the modelled velocity variability is significantly smaller and the phasing of the modelled velocity variability is offset by a couple of months compared to the GNSS measurements for all basal melt perturbations (Figure 4). Additionally, for Site 4 the modelled velocity variability has a similar phasing to the GNSS measurements, but an 80 m/a basal melt perturbation is needed to model a similar amplitude in velocity variability. This may indicate that a combination of mechanisms may be driving these velocity variations at Sites 3 and 4. We also show that seasonal variability in SSH alone cannot reproduce the two velocity peaks observed at the new GNSS sites (Sites 1, 2 and 4).

In the modelling experiments, basal melt rates that peak in October and April are required to reproduce the observed velocity peaks in austral summer (December and/or January) and austral winter (June and/or July) at Sites 1, 2 and 4 (Figures 2 and 4). Our modelled basal melt perturbations highlight that there is a delay of 2-3 months between the peak basal melt rates and



405 velocities. We suggest this delay is due to the time it takes for the basal melt rates to thin the ice shelves significantly enough to change the stress regime at the GNSS sites. Previous studies have found that lag times in the ice shelf flow response occur due to the time required for basal melting to cause sufficient thinning (thickening) to produce an observable acceleration (deceleration) of the ice shelf. We suggest that the time delay between basal melting and velocity change depends on the proximity of the region of interest to the highest basal melt rates and the thickness of that region (i.e., thicker areas have a greater lag time). In this study, we are perturbing basal melt rates at identified sensitive regions of the ice shelf that exist both locally and up to 1000 km away from uniformly everywhere, as has been done previously, we only perturb basal melt rates at identified sensitive regions of the ice shelf. Our sensitivity maps highlight that very local perturbations in basal melt can have a significant effect on the ice flow speed, sometimes 1000km away from GNSS sites (Figure A53). We hypothesize that the velocities reach a maximum in austral summer (December and/or January) and austral winter (July and/or June) as the ice within these sensitive regions has thinned significantly during periods of peak melting in October and April (Figures 2 and 4). We also found that the Totten Ice Shelf velocity maxima occurs at the end of the high melt season in July when the ice thickness reaches a minimum.

Sensitive regions identified from the AD experiments are located often at or near pinning points (Figures A5, A6 and A7). Such areas are important for ice shelf stability and buttressing. Figure 3 shows that velocities at find that GNSS Sites 1, 2, and 3 are most sensitive to basal melt rate perturbations at local perturbations in basal melt rates near the Ross Island region pinning point. Previous studies have shown that Ross Island is an important pinning point for the RIS, with changes in ice thickness here found to significantly impact overall ice shelf dynamics (Reese et al., 2018; Gudmundsson et al., 2019). On floating ice shelves, basal drag is negligible and the lateral drag depends on the existence of ice shelf margins and/or pinning points. Ice shelf thinning can reduce the thickness of shear margins and the contact area over pinning points and ice rises, which decreases the lateral drag and the buttressing ability of the ice shelf. This reduction in buttressing has a near-instantaneous effect on ice shelf acceleration buttressing force exerted by these pinning points (Larter, 2022; Arndt et al., 2018; Joughin et al., 2021; Dupont and Alley, 2005; Gudmundsson et al., 2019). also observed that ice shelf thinning (thickening) was coincident with faster (slower) velocities due to changes in resistive stresses at ice rumples present on the Totten Ice Shelf Our sensitivity maps confirm this finding, highlighting that Sites 1, 2 and 3 ice speeds are highly sensitive to local changes in basal melt at the calving front near the Ross Island pinning point.

430 Additionally, we perturb Furthermore, we find that at GNSS Site 4, ice speed is most sensitive to local perturbations in basal melt rates at the KIS grounding zone to try and reproduce the intra-annual velocity signal at Site 4. with changes in basal melt elsewhere on the ice shelf having almost no impact on ice speed at this site. Changes in basal melting near the grounding zones generally lead leads to ice thinning and grounding line retreat (Baldacchino et al., 2022; Ranganathan et al., 2021). This can cause changes in basal stresses, ice velocities, and discharge of the ice stream and/or outlet glacier, which induces an increase in flow speed. Additionally, ice thinning reduces the buttressing effect from ice rises downstream of the KIS grounding zone, which drive changes in the velocities at Site 4 and elsewhere on the ice shelf.

#### 4.2 ~~Comparison to observed~~ Magnitude of variability

~~We perturb the basal melt rates beneath the Ross Ice Shelf. The basal melt rates used in this study are high for the Ross Ice Shelf today, however, our focus here is on asking whether perturbations in basal melt rates can reproduce a similar velocity variability as observed by the GNSS units. We found that seasonal perturbations in basal melt rates (with a magnitude of 20 m/a) can reproduce a similar velocity variability for Sites 1 and 2. Our AD-inferred sensitivity map shows that we do not need 20 m/a of perturbation under the entire ice shelf, but only over 2% of the ice shelf (i.e., identified sensitive regions). In this section, we suggest that the melt rate perturbations used in our modelling experiments are more probable for Sites 1 and 2 than for Sites 3 and 4.~~

445 ~~Firstly, we perturbed the basal melt rates to peak in April and October to reproduce~~ match the observed intra-annual velocity variability on the ice shelf (Figures 2 and 4). ~~displays Current basal melt observations display~~ large variability in basal melt rates throughout the year ~~near at~~ the calving front ~~of the RIS, observes a near~~ Ross Island, with large basal melt ~~peak peaks~~ in the austral summer (January - March) ~~of~~ > 3 m/a and smaller basal melt peaks in early ~~winter~~ (April and/or May) and late ~~austral~~ winter (October and/or November) of 1-2 m/a ~~at the calving front near the Ross Island pinning point. Additionally, observe that the basal melt rates during winter are an order of magnitude higher than the satellite measured ice shelf average. They suggest that these higher basal melt rates during the~~ (Stewart et al., 2019; Jendersie et al., 2018; Årthun et al., 2013). ~~These basal melt peaks in the~~ early winter are due to the remnant heat from the summer AASW inflow and in late winter are due to the inflows of HSSW into the ice shelf cavity when large heat loss and sea ice production leads to active cross-frontal flow that ventilates the cavity (Stewart et al., 2019; Jendersie et al., 2018; Årthun et al., 2013). ~~Figure A8 also shows the large variability in the baseline MITgem basal melt rates similar to the observations made by , highlighting that basal melt rates have more variability than presented in . Additionally, suggests that the actual total summer increase in the heat content of the AASW layer near the ice front is likely to be larger than their modelled increase~~ These smaller basal melt peaks in early and late austral winter align with the sinusoidal phasing of our idealized basal melt perturbations. However, we do not capture the variability in basal melt during the rest of the year, and the ~~seasonal enhancement of the basal melting will continue further into autumn than in their model. extended the late melt period to April and found that this also shifted the timing of maximum velocity a month later, suggesting that a longer or later melt period at the front could have aligned their modelled and observed velocity phases similar to our results in this study. These findings support the timing of our significantly larger basal melt peaks observed in the austral summer (January - March) (Stewart et al., 2019) (Figures A8 and A9). Therefore, our idealized sinusoidal perturbed basal melt rate peaks in April and October at the calving front near Ross Island which influences the velocities at Sites 1, 2, and 3. rates do not align with current observations of basal melting on the RIS.~~

465 ~~Secondly~~ Additionally, we perturb the basal melt rates with a range of magnitudes (~~20-80~~ 20 - 80 m/a) to try and ~~reproduce the observed velocity variability at the GNSS sites. We match the observed intra-annual velocity variability on the ice shelf. Our results show that we need to~~ perturb the basal melt rates near the Ross Island shear zone by a magnitude of 20 m/a for Sites 1 and 2 to ~~reproduce intra-annual velocity variations similar to the GNSS measurements~~ match the GNSS observations (Figures 3, 2 and 4). ~~Our AD-inferred sensitivity map shows that we do not need 20 m/a of perturbation under the entire ice shelf, but only over 2% of the ice shelf (i.e., identified sensitive regions).~~ The RIS has low annual average basal melt rates across the ice shelf (~~0-10~~ 0 - 1 m/a), with the highest average basal melt rates observed at the ice shelf front (> 3 m/a), near Ross

Island pinning point (Stewart et al., 2019; Stevens et al., 2020; Das et al., 2020; Adusumilli et al., 2020; Schodlok et al., 2016; Assmann et al., 2003; Holland et al., 2003; Stern et al., 2013). ~~Figure ?? shows that MITgem maximum summer basal melt rates along the calving front are 10-25 m/a, which is similar to our basal melt perturbation of 20 m/a for Sites 1 and 2. Recently~~  
475 Stewart et al. (2019) ~~also observed~~ has observed high austral summer basal melt rates of ~~10-50~~ 10 - 50 m/a at the calving front near Ross Island, due to the seasonal inflow of summer-warmed AASW from the adjacent Ross Sea Polynya downwelling into the ice shelf cavity. However, ~~the modelled (Figure ??) and observed basal melt magnitudes of 20 m/a~~ these observed higher basal melt rates occur during the austral summer, and we perturb basal melt rates with magnitudes of  $> 20$  m/a in early and late austral winter.

480 ~~However, for Site 3, none of the basal melt perturbations were able to reproduce intra-annual velocity variations similar to the GNSS measurements. This suggests that if melt is responsible then larger perturbations may be needed at the identified sensitive regions to reproduce the observed velocity variability. However, basal melt magnitudes of  $> 80$  m/a are highly unrealistic for the RIS today. Therefore, we suggest that Site 3's current observed intra-annual velocity variations may be driven by a combination of mechanisms not captured by our model.~~

485 ~~MITgem summer maximum and mean basal melt rates (in m/a) on the RIS.~~

~~Additionally, for Site~~ For Site 4 we perturb ~~also need to perturb the~~ basal melt rates with ~~magnitudes of~~ significantly high magnitudes (80 m/a) at the KIS grounding zone and Siple Coast ice rises to ~~reproduce intra-annual velocity variability. Perturbed basal melt magnitudes of 80 m/a are unrealistically high match the GNSS observations. Observed basal melt rates are low~~ for the interior of the ice shelf, ~~with observed basal melt rates being low (0-1 m/a). Localised~~, with localised high  
490 basal melt rates of  $22.2 \pm 0.2$  m/a ~~have been~~ observed near grounding lines of the Siple Coast Ice Streams. ~~However, no~~ (Marsh et al., 2016; Adusumilli et al., 2020). These studies show that the magnitudes that we use to perturb the basal melt rates ~~of 80 on the RIS are significantly higher than observed, which may indicate that our perturbation is not realistic. Additionally, our perturbation represents a sine function, and thus it peaks and troughs at the same magnitudes (i.e., peaks at 25 m/a, and troughs at -25 m/a have been observed on seasonal timescales at the Siple Coast grounding lines or pinning points and ice~~  
495 rises. ~~Seasonally pronounced basal melt predominantly occurs along the RIS front, with and observing that the seasonal basal melt rates decrease with distance from the calving front. The interior of the ice shelf has a residence time of 1-6 years for sub-ice shelf waters resulting in a~~ to include both melting and refreezing (Figure A9). These negative basal melt rates ~~varying on much longer timescales. Therefore, it is unlikely that Site 4's observed intra-annual velocities are driven by seasonal changes in basal melt rates (i.e., refreezing) are significantly higher than expected for the RIS, especially in the summer (Figures A8 and  
500 A9) (Stewart et al., 2019).~~

~~We also perturb~~ Our findings indicate that basal melt rates ~~at the Siple Coast pinning points and ice rises to reproduce intra-annual velocity variations at Site 2. It is unlikely that seasonally varying basal melt rates at the Siple Coast pinning points and ice rises are only capable of causing the observed velocity variations after we apply our idealized sinusoidal perturbations. As the required perturbations are significantly higher than expected, it is likely that other mechanisms are driving the velocity~~  
505 ~~variations at Site 2. We suggest that the seasonal basal melt variability observed at the calving front is driving the majority of Site 2's intra-annual velocity variability (Figure 4).~~

### 4.3 ~~Other potential drivers of intra-annual velocity variability~~

~~We highlight that seasonal changes in basal melt can reproduce the observed intra-annual velocity variations at Sites 1 and 2, using perturbed basal melt rates with magnitudes of 20-observed velocity variations. However, we highlight if melt alone was responsible, and it occurred only at sensitive regions of the ice shelf, then variability in basal melting with peaks in April and October, and magnitudes of 20-80 m/a at the calving front. Our study differs from due to : (1) our new GNSS datasets for are needed to match the GNSS observations at Sites 1 and 2 displaying two velocity peaks per year, whereas Site 3 only displayed one velocity peak per year, (2) we use weekly MITgem basal melt rates which can capture intra-annual variability in atmospheric, oceanic and sea-ice conditions in the Ross Sea and (3) we use the AD model to identify sensitive areas of the ice shelf, and then perturb basal melt rates at these sensitive areas and 4.~~

### 4.3 Other potential drivers of variability

We can match GNSS observations at Sites 1, 2 and 4 when applying our idealized sinusoidal basal melt perturbations at identified sensitive regions. However, we ~~also highlight that seasonal changes in basal melt cannot reproduce the observed intra-annual velocity variations at are unable to do so for Site 3, which is~~ consistent with the findings conclusions of Klein et al. (2020). Additionally, for Site 4, we were able to reproduce the observed intra-annual velocity variations using an extremely high perturbed basal melt rate of 80 m/a at the KIS grounding zone and ice rises downstream of the Siple Coast ice streams, where no evidence of seasonally high basal melting rates has been observed. Therefore, in this section, we discuss other potential drivers of the observed intra-annual velocity variability at Sites 3 and 4. Here we list some other possible drivers.

Most recently, Mosbeux et al. (2023) has shown that the seasonal variability of sea surface height (SSH) modifies ice velocity by changing (1) the driving stress by locally tilting the ice shelf and (2) the basal condition in the grounding zone. ~~However, we show~~ Our results indicate that seasonal variability in SSH alone cannot reproduce the two velocity peaks per year observed at our new GNSS sites. We suggest that Mosbeux et al. (2023) ~~was were~~ able to reproduce the velocity variability recorded at Site 3 due to implementing additional parameterization of viscoelastic processes in their model. However, we find a closer similarity in velocity amplitudes at Sites 2, 3 and 4 to the GNSS measurements when forced by changes in SSH compared to basal melt. Therefore, seasonal variations in SSH are likely ~~providing a small additional contribution contributing~~ to velocity changes on the RIS as indicated by Mosbeux et al. (2023) ~~and shown by the similarity in velocity amplitudes at Sites 3 and 4 to the GNSS measurements.~~

~~Additionally,~~ Greene et al. (2018) found that changes in buttressing from sea ice can explain the seasonal cycle of Totten Glacier's ice shelf velocities. Sea ice cover in the Ross Sea decreases in the ~~summer months~~ austral summer and increases in the ~~winter months~~ austral winter, suggesting that ice shelf velocities would increase in the austral spring and decrease in the austral winter if forced by variations in sea ice backstress (Greene et al., 2018; Cassotto et al., 2015; Howat et al., 2010). However, we observe an acceleration in ice shelf velocities in austral summer and austral winter, indicating that the GNSS velocity variations are likely not forced by variations in sea ice backstress.

Seasonal variations in surface air temperatures can also influence the surface melt rates of the ice shelf (Nicolas et al., 2017a; Trusel et al., 2015; Zou et al., 2021a, b) and drive variations in velocities. For example, it has been shown that surface meltwater influences ice shelf velocity by percolating through and weakening the ice shelf shear margins (Cavanagh et al., 2017; Liu and Miller, 1979; Vaughan and Doake, 1996; Greene et al., 2018; Alley et al., 2018). However, the surface melt rates on the RIS are small, and the response of the ice shelf velocities to summer elevated surface melting has been shown to occur over short timescales (hours to weeks) (Stevens et al., 2022; Chaput et al., 2018; Nicolas et al., 2017a). An El-Niño event occurred in the summer of 2015/2016 when the GNSS measurements for Site 3 were recorded. This event may have increased surface melt rates on the RIS as well as modified wind patterns and ocean circulation (Klein et al., 2020; Paolo et al., 2015). Nicolas et al. (2017b) observed 14 days of enhanced surface melting on the RIS, between the 10th and 21st of January 2016 due to persistent air temperatures higher than  $-2^{\circ}\text{C}$  in the region of Site 3 (Klein et al., 2020; Chaput et al., 2018). Klein et al. (2020) suggests that the surface heat fluxes over the ocean during this surface melt event may have been substantially different than those used to drive the ocean models. Therefore, the MITgcm basal melt rates likely do not take into account this high surface melt event and this may explain why we cannot reproduce the intra-annual velocity variability observed at Site 3.

Tides are known to cause substantial variations in velocity over short periods (Anandakrishnan et al., 2003; Gudmundsson, 2006; Bindschadler et al., 2003) and longer periods of up to a year (Murray et al., 2007). However, Klein et al. (2020) highlighted that the vertical signals of tides are too small to provide a significant forcing to the horizontal movement of the RIS through non-linear ice-ocean processes along the grounding zone as suggested by Murray et al. (2007). Our GNSS processing smooths out short-term tidal effects, but daily variability is likely to be large, with the Ross Sea tides being almost diurnal (Brunt et al., 2010; Padman et al., 2003). Therefore, small, solar-annual, or semi-annual (equinox) tides may drive the remaining variability in velocities observed at the GNSS sites that our model perturbations are unable to reproduce. Additionally, Mosbeux et al. (2023) observed a 6-month signal in their GNSS datasets on the RIS and tentatively attributed this signal to semiannual changes in tides. This 6-month tidal signal may explain the observed intra-annual velocity variability at Site 4, and we suggest that it is likely that the tidal signal is playing a role in observed velocity variability at all GNSS sites.

Flow variability in the Siple Coast Ice Streams has also been shown to occur on short timescales due to changes in the distribution and supply of basal meltwater (Catania et al., 2012). Recently, high basal melt rates of 35 m/a have been inferred at the KIS grounding zone within a narrow subglacially sourced basal channel (Whiteford et al., 2022). These high basal melt rates within a subglacial channel suggest that meltwater plumes could be driving changes in the subglacial hydrology system of the KIS. These changes in the subglacial hydrology may be driving variations in the velocities on intra-annual timescales by modifying the basal friction at the KIS grounding line. However, further work is needed to investigate these observed intra-annual velocity variations at Site 4, which is outside the scope of this study.

## 5 Conclusions

We ~~tested the hypothesis that seasonal perturbations in basal melt can reproduce~~ set out to further understand the drivers of intra-annual velocity variability ~~recorded at four long-duration GNSS stations on the Ross Ice Shelf (RIS) using ISSM.~~

~~We presented on the Antarctic ice shelves, using the RIS as a testbed. We present~~ three new GNSS datasets that display an intra-annual velocity variability (two velocity peaks per year) that ~~has have~~ not yet been explored in previous studies (Klein et al., 2020; Mosbeux et al., 2023). ~~We found that by perturbing basal melt rates at identified sensitive regions~~ Notably, our  
575 ~~new observations display a consistent periodicity that is different to previous year-round velocity observations from the Ross Ice Shelf. We investigate the potential role of basal melt variability on the RIS ice flow by (1) identifying regions where changes in melt would have the largest impact on ice speed at our GNSS sites and (2) applying idealized sinusoidal basal melt perturbations at these sensitive regions to identify what magnitude of variability is needed to match the GNSS observations. We find that localized changes in basal melt can have a strong impact on the ice shelf~~ ~~we can reproduce similar intra-annual velocity variations to the GNSS measurements~~ flow. Our sensitivity maps highlight that the pinning points and grounding lines of the RIS are highly sensitive to changes in basal melting, and have an impact on ice shelf flow speed. Additionally, we identify the magnitude of variability needed to match the GNSS observations of velocity change at the GNSS sites. We are able to match the GNSS observations at Sites ~~1 and 2~~, 2 and 4 using our idealized sinusoidal basal melt perturbations with magnitudes of 20-80 m/a. However, the required basal melt perturbations are significantly higher than expected for the RIS,  
585 ~~which may indicate that these perturbations are not realistic. Therefore isolated regions of periodically-high basal melting are unlikely to be the main factor driving observed GNSS velocity variability.~~ We also show that seasonal variability in SSH alone cannot reproduce the intra-annual velocity variability observed at the new GNSS sites. However, it is likely that changes in SSH and tides in the Ross Sea are contributing to the observed variability in velocities at all GNSS sites. ~~We~~ Therefore, we suggest that a combination of external forcings ~~and internal mechanics~~ (e.g. SSH and tides) and internal mechanics (e.g. changes in  
590 ~~buttressing forcings and basal friction~~) may be at play to produce the observed intra-annual velocity variability ~~at Sites 3 and 4.~~

We suggest that future work could focus on (1) continuing and expanding the multi-year GNSS records of seasonally resolved ice velocity changes on the RIS, (2) examining ice shelf interactions with basal melt rates on floating and grounded ice through coupled ocean-ice shelf models, and (3) ~~exploration of exploring~~ other potential drivers of intra-annual velocity  
595 variations ~~particularly concerning the observed seasonal velocity variations at the KIS grounding zone.~~

~~Our results highlight that seasonal perturbations in basal melt rates can reproduce GNSS-observed velocity variability in some cases, although the perturbations required in our study are large. The observed intra-annual velocity variations at all GNSS sites are likely driven by a complex combination of external forcings and internal mechanics on the RIS. However, our sensitivity maps highlight where increases in basal melt rates will influence ice velocity today and in the future. Specifically, the sensitive regions identified at the calving front near the Ross Island pinning point are already undergoing significant seasonal increases in basal melt rates. Our AD-inferred sensitivity map shows that we do not need 20 m/a of perturbation under the entire ice shelf, but only over 2% of the ice shelf to reproduce the intra-annual velocity variations at Sites 1 and 2. Therefore, we are likely to observe continued intra-annual velocity variations on the RIS driven by seasonal changes in basal melting at the calving front.~~

600

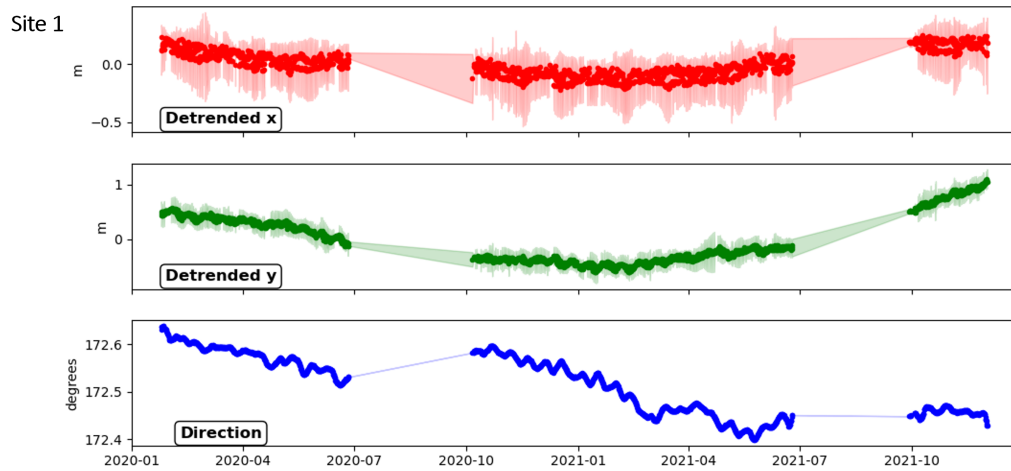


**Figure A1.** Site 1 GNSS detrended position (x, y) and direction (clockwise from grid north).

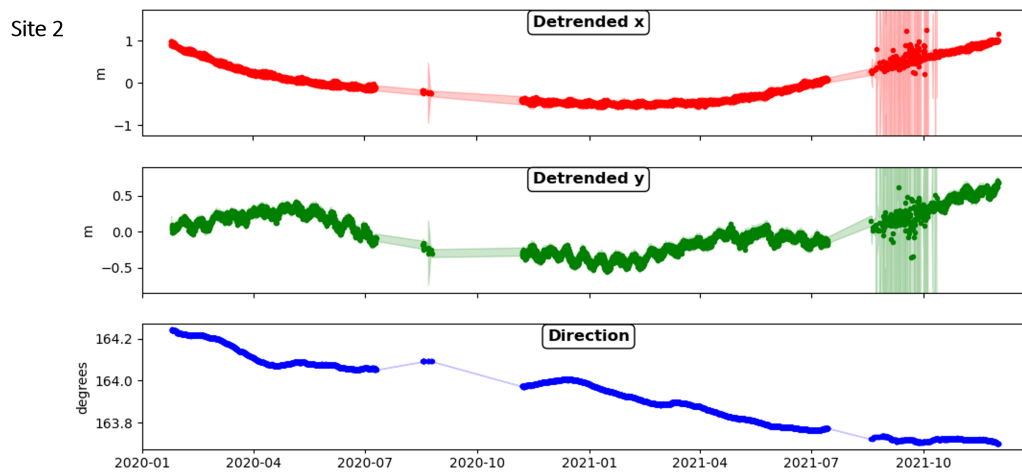


**Figure A2.** Site 2 GNSS detrended position (x, y) and direction (clockwise from from grid north).

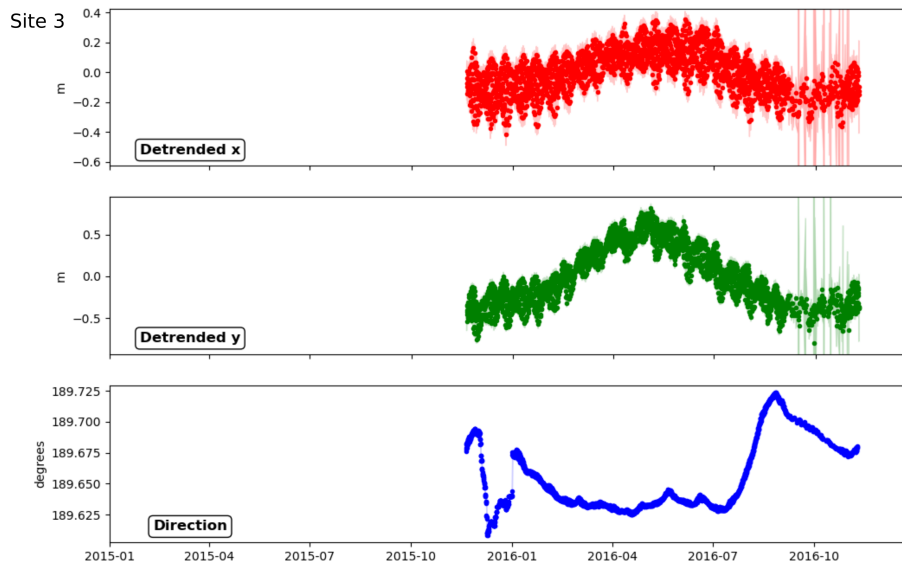


**Figure A3.** Site 3 GNSS detrended position (x, y) and direction (clockwise from grid north).

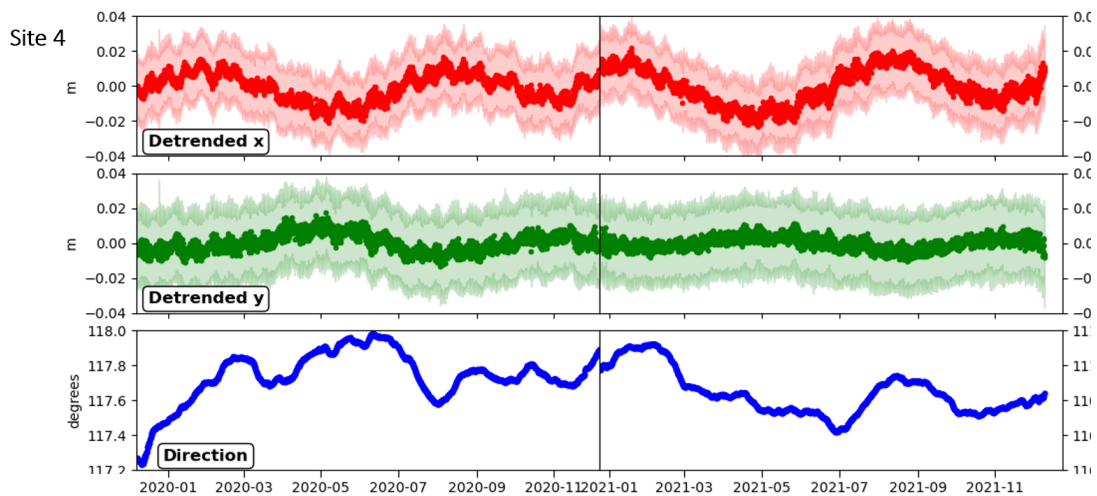


**Figure A4.** Site 4 GNSS detrended position (x, y) and direction (clockwise from from grid north).



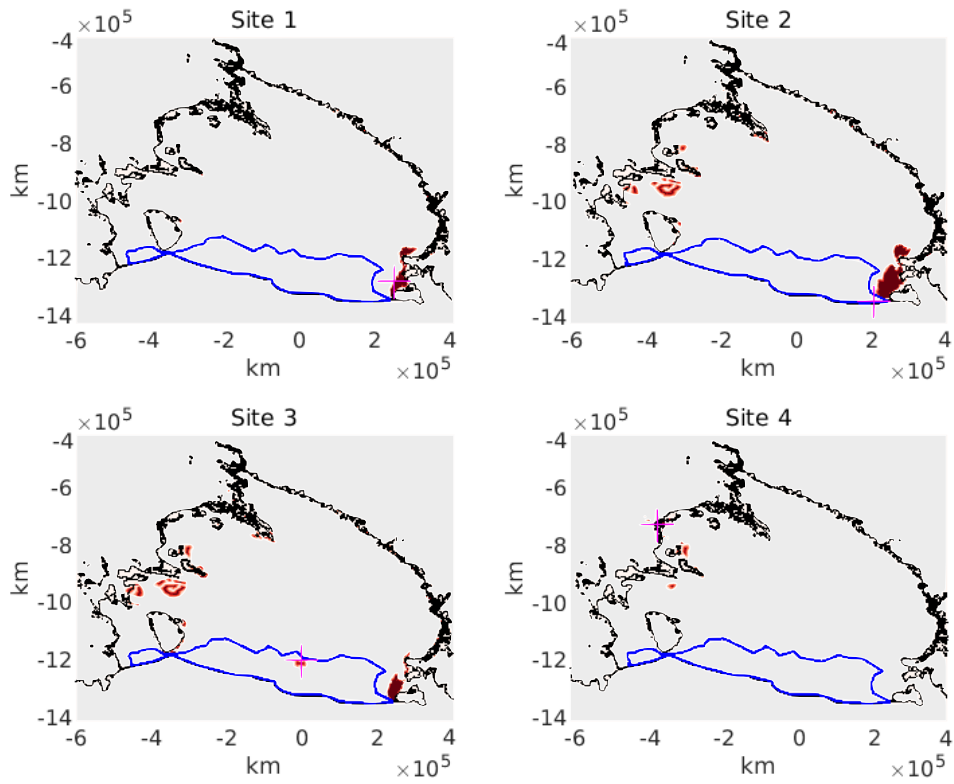


**Figure A5.** Locations where the idealized sinusoidal basal melt rate was perturbed seasonally (i.e., where perturbations were applied when the AD mapped sensitivity is greater than threshold was set to  $2e-11 \text{ m}^{-2}$ ) (dark red) for each GNSS site (pink markers). The grounding line (black line) and passive ice (blue line) on the RIS identified by Fürst et al. (2016) are highlighted.

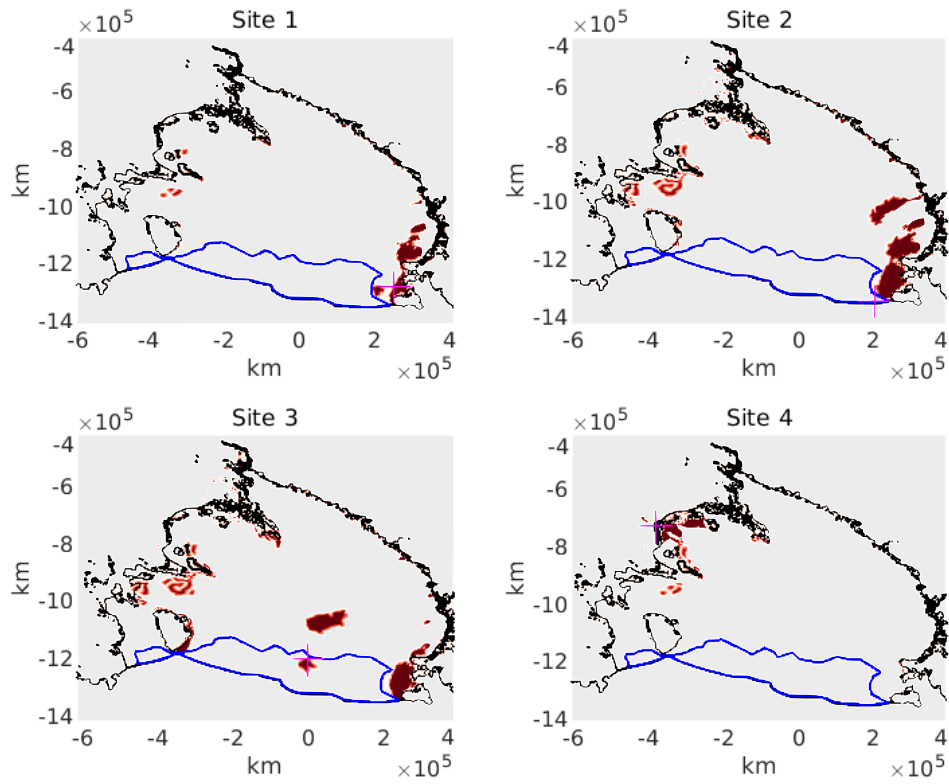


**Figure A6.** Locations where the idealized sinusoidal basal melt rate is perturbed seasonally (i.e., where perturbations were applied when the AD mapped sensitivity is greater than threshold was set to  $0.5e - 11 \text{ m}^{-2}$  (highlighted in dark red)) for each GNSS site (pink marker). The grounding line (black line) and passive ice (blue line) on the RIS identified by Fürst et al. (2016) are highlighted.

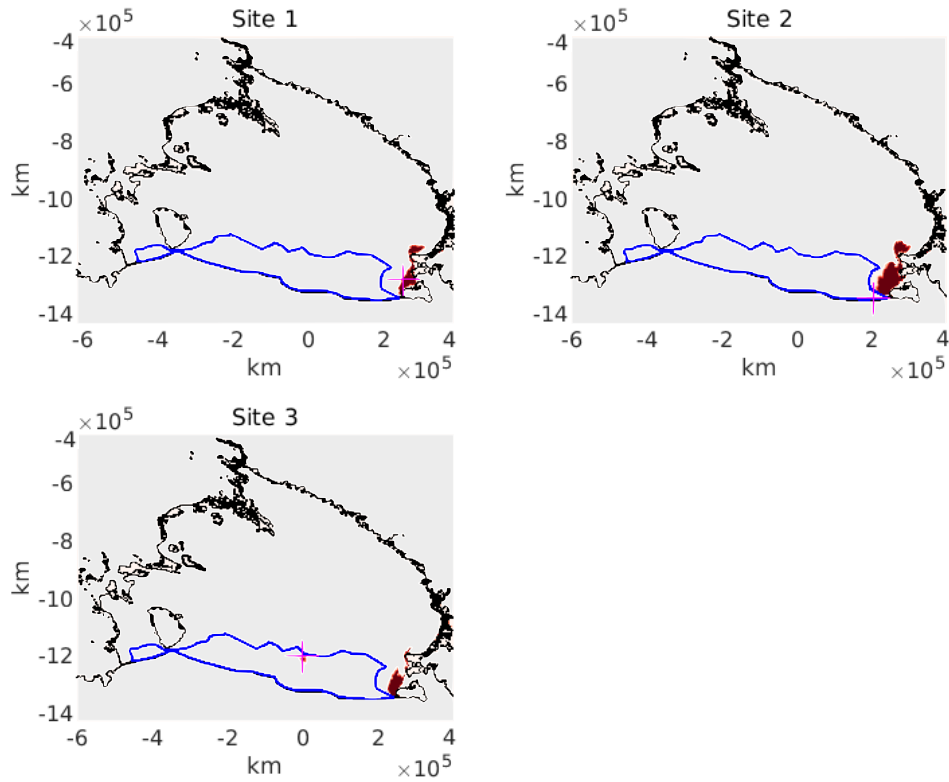


**Figure A7.** Locations where the idealized sinusoidal basal melt rate is perturbed seasonally (i.e., where perturbations were applied when the AD mapped sensitivity is greater than threshold was set to  $2e - 11 \text{ m}^{-2}$  and located along limited to the calving front close to the Ross Island pinning point (highlighted in dark red ) for GNSS Sites 1, 2 and 3 (pink marker). The grounding line (black line) and passive ice (blue line) on the RIS identified by Fürst et al. (2016) are highlighted.

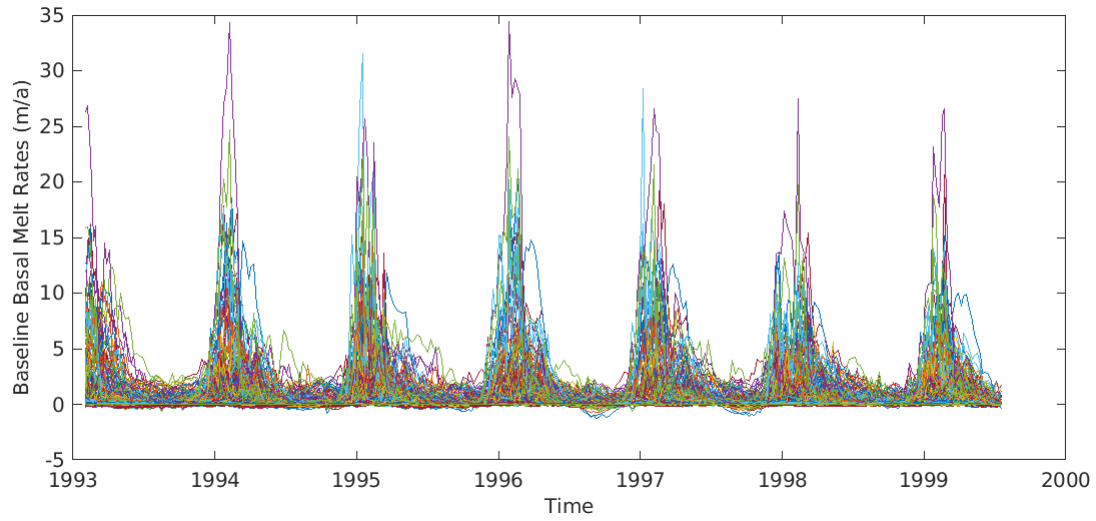


**Figure A8.** The baseline MITgcm basal melt rates for the identified sensitive regions (greater than  $2e - 11 \text{ m}^{-2}$ ) on the RIS. Each coloured line represents a different sensitive region.

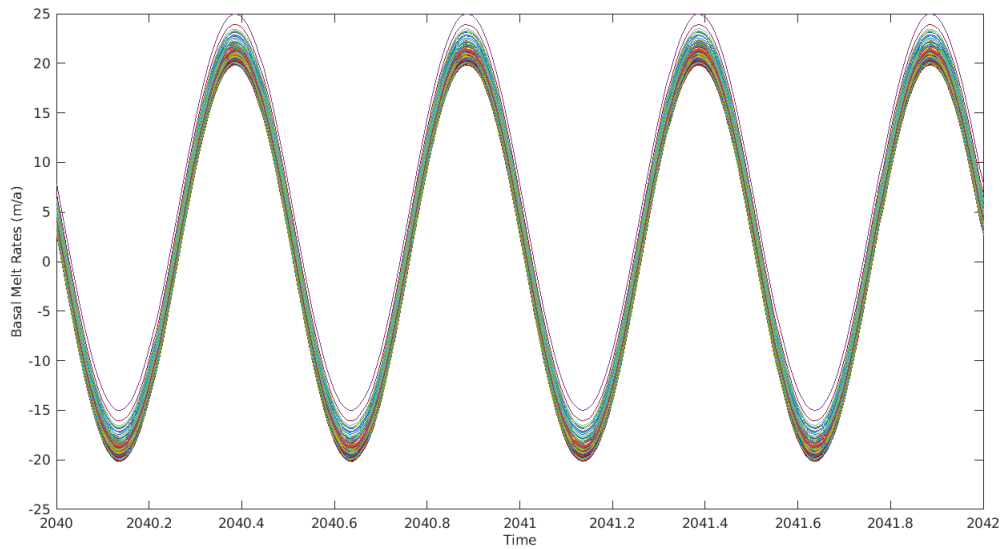


**Figure A9.** The idealized sinusoidal perturbed MITgcm basal melt rates for-at the identified sensitive regions (greater than  $2e - 11 \text{ m}^{-2}$ ) on the RIS. Each coloured line represents a different sensitive region.

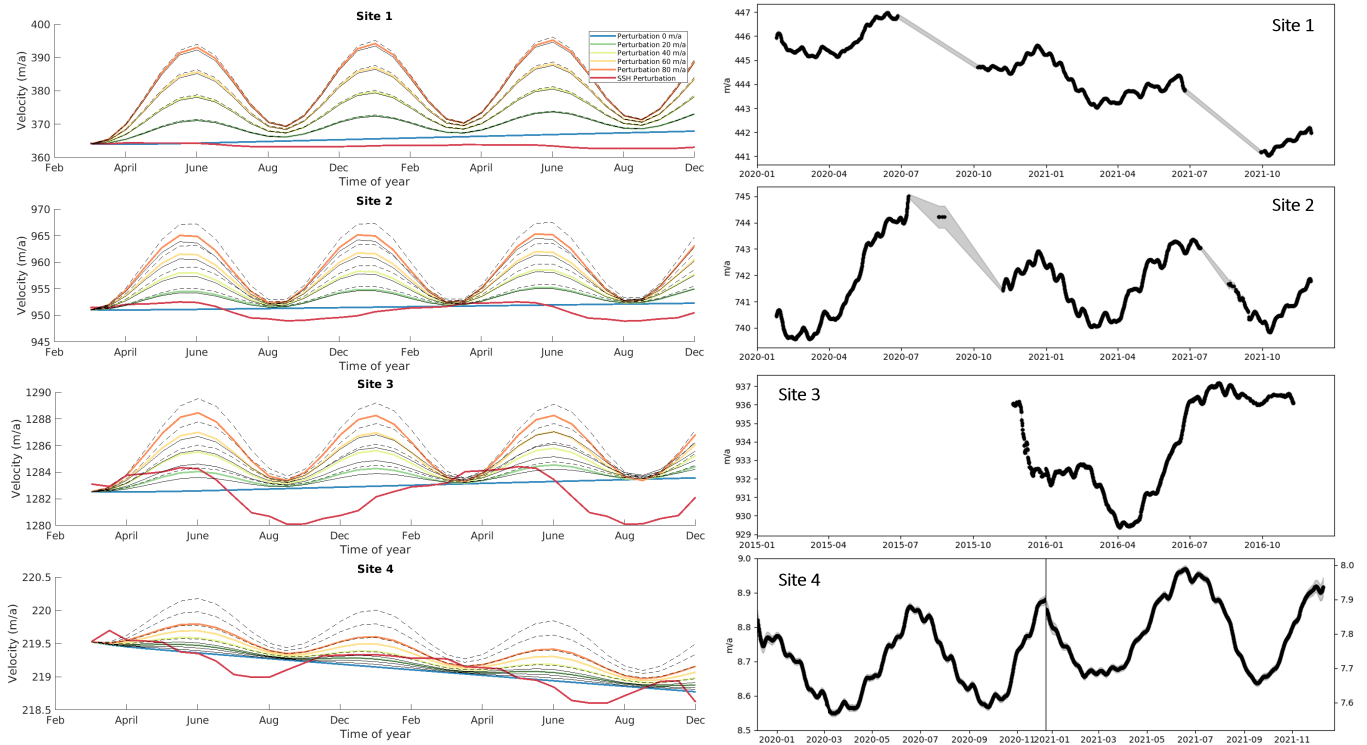


**Figure A10.** The absolute modelled velocities compared to the absolute GNSS observed velocities for Sites 1, 2, 3, and 4.

*Data availability.* The model scripts and configuration files used in this study can be found here <https://doi.org/10.5281/zenodo.11098089>. The Ice-sheet and Sea-level System Model v4.18 can be accessed at <https://issm.jpl.nasa.gov>. BedMachine Antarctica is available at NSIDC (<http://nsidc.org/data/nsidc-0756>). InSAR-Based ice velocity is found at NSIDC (<https://nsidc.org/data/nsidc-0484/>). The Antarctic surface mass balance (RACMO 2.3p2) is available at <https://www.projects.science.uu.nl/iceclimate/models/racmo-data.php>. GNSS data will be up-  
610 loaded to a suitable repository (Zenodo) on acceptance.

*Author contributions.* Project vision, funding acquisition and field planning (2019/20 season) was led by Nicholas Golledge. The event leader for field season 2021/2022 was Alanna V. Alevropoulos-Borrill. Field assistants for fieldwork included Francesca Baldacchino, Laurine van Haastrecht, Dan Lowry, and Alexandra Gossart. Site 4 data acquisition and GNSS processing of all sites was carried out by Huw Horgan. GNSS analysis was carried out by Francesca Baldacchino and Huw Horgan. ISSM simulations and AD analysis were carried out by Francesca  
615 Baldacchino under the guidance of Mathieu Morlighem. AD simulations were carried out by Mathieu Morlighem. MITgcm basal melt outputs were provided by Alena Malyarenko. All authors contributed to the manuscript.

*Competing interests.* Huw Horgan is an associate editor for The Cryosphere and EGU sphere. The authors declare that they have no other conflicts of interest.

*Acknowledgements.* We are grateful to Antarctic New Zealand for facilitating and supporting our field campaigns to the Ross Ice Shelf to  
620 install and collect GNSS measurements. Additionally, we are grateful to Peter Bromirski for sharing the raw GNSS datasets collected on the Ross Ice Shelf in 2015-2016 that have been included in this study. This work was supported by the New Zealand Ministry for Business, Innovation and Employment contracts RTUV1705 (“NZSeaRise”) and ANTA1801 (“Antarctic Science Platform”), and Royal Society of New Zealand contracts VUW-1501 and VUW16-02.

## References

- 625 Adusumilli, S., Fricker, H. A., Medley, B., Padman, L., and Siegfried, M. R.: Interannual variations in meltwater input to the Southern Ocean from Antarctic ice shelves, *Nature Geoscience*, 13, 616–620, <https://doi.org/10.1038/s41561-020-0616-z>, 2020.
- Agosta, C., Amory, C., Kittel, C., Orsi, A., Favier, V., Gallée, H., van den Broeke, M. R., Lenaerts, J. T. M., van Wessem, J. M., van de Berg, W. J., and Fettweis, X.: Estimation of the Antarctic surface mass balance using the regional climate model MAR (1979–2015) and identification of dominant processes, *The Cryosphere*, 13, 281–296, <https://doi.org/10.5194/tc-13-281-2019>, 2019.
- 630 Alley, K. E., Scambos, T. A., Anderson, R. S., Rajaram, H., Pope, A., and Haran, T. M.: Continent-wide estimates of Antarctic strain rates from Landsat 8-derived velocity grids, *Journal of Glaciology*, 64, 321–332, <https://doi.org/10.1017/jog.2018.23>, 2018.
- Anandakrishnan, S., Voigt, D., Alley, R., and King, M.: Ice stream D flow speed is strongly modulated by the tide beneath the Ross Ice Shelf, *Geophysical Research Letters*, 30, 2003.
- Arndt, J. E., Larter, R. D., Friedl, P., Gohl, K., Höppner, K., et al.: Bathymetric controls on calving processes at Pine Island Glacier, *The*
- 635 *Cryosphere*, 12, 2039–2050, 2018.
- Årthun, M., Holland, P. R., Nicholls, K. W., and Feltham, D. L.: Eddy-driven exchange between the open ocean and a sub-ice shelf cavity, *Journal of Physical Oceanography*, 43, 2372–2387, 2013.
- Assmann, K., Hellmer, H. H., and Beckmann, A.: Seasonal variation in circulation and water mass distribution on the Ross Sea continental shelf, *Antarctic Science*, 15, 3–11, <https://doi.org/10.1017/S0954102003001007>, 2003.
- 640 Baldacchino, F., Morlighem, M., Golledge, N. R., Horgan, H., and Malyarenko, A.: Sensitivity of the Ross Ice Shelf to environmental and glaciological controls, *The Cryosphere*, 16, 3723–3738, <https://doi.org/10.5194/tc-16-3723-2022>, 2022.
- Bindschadler, R. A., Vornberger, P. L., King, M. A., and Padman, L.: Tidally driven stick-slip motion in the mouth of Whillans Ice Stream, Antarctica, *Annals of Glaciology*, 36, 263–272, <https://doi.org/10.3189/172756403781816284>, 2003.
- Bougamont, M., Christoffersen, P., Price, S., Fricker, H. A., Tulaczyk, S., and Carter, S. P.: Reactivation of Kamb Ice Stream tributaries
- 645 triggers century-scale reorganization of Siple Coast ice flow in West Antarctica, *Geophysical Research Letters*, 42, 8471–8480, 2015.
- Brunt, K. M.: Tidal motion of the Ross Ice Shelf and its interaction with the Siple Coast ice streams, Antarctica, The University of Chicago, 2008.
- Brunt, K. M. and MacAyeal, D. R.: Tidal modulation of ice-shelf flow: A viscous model of the Ross Ice Shelf, *Journal of Glaciology*, 60, 500–508, <https://doi.org/10.3189/2014JoG13J203>, 2014.
- 650 Brunt, K. M., King, M. A., Fricker, H. A., and MacAyeal, D. R.: Flow of the Ross Ice Shelf, Antarctica, is modulated by the ocean tide, *Journal of Glaciology*, 56, 157–161, <https://doi.org/10.3189/002214310791190875>, 2010.
- Cassotto, R., Fahnestock, M., Amundson, J. M., Truffer, M., and Joughin, I.: Seasonal and interannual variations in ice mélange and its impact on terminus stability, Jakobshavn Isbræ, Greenland, *Journal of Glaciology*, 61, 76–88, <https://doi.org/10.3189/2015JoG13J235>, 2015.
- 655 Catania, G., Hulbe, C., Conway, H., Scambos, T. A., and Raymond, C.: Variability in the mass flux of the Ross ice streams, West Antarctica, over the last millennium, *Journal of Glaciology*, 58, 741–752, 2012.
- Cavanagh, J., Lampkin, D., and Moon, T.: Seasonal variability in regional ice flow due to meltwater injection into the shear margins of Jakobshavn Isbræ, *Journal of Geophysical Research: Earth Surface*, 122, 2488–2505, 2017.

- Chaput, J., Aster, R., McGrath, D., Baker, M., Anthony, R. E., Gerstoft, P., Bromirski, P., Nyblade, A., Stephen, R., Wiens, D., et al.: Near-surface environmentally forced changes in the Ross Ice Shelf observed with ambient seismic noise, *Geophysical Research Letters*, 45, 11–187, 2018.
- Cuffey, K. M. and Paterson, W. S. B.: *The physics of glaciers*, Academic Press, 2010.
- Das, I., Padman, L., Bell, R. E., Fricker, H. A., Tinto, K. J., Hulbe, C. L., Siddoway, C. S., Dhakal, T., Frearson, N. P., Mosbeux, C., Cordero, S. I., and Siegfried, M. R.: Multidecadal Basal Melt Rates and Structure of the Ross Ice Shelf, Antarctica, Using Airborne Ice Penetrating Radar, *Journal of Geophysical Research: Earth Surface*, 125, <https://doi.org/10.1029/2019JF005241>, 2020.
- Davis, P. and Nicholls, K.: Turbulence observations beneath Larsen C Ice Shelf, Antarctica., *J. Geophys. Res.*, 124, 5529–5550, <https://doi.org/10.1029/2019jc015164>, 2019.
- Depoorter, M. A., Bamber, J. L., Griggs, J. A., Lenaerts, J. T., Ligtenberg, S. R., Van Den Broeke, M. R., and Moholdt, G.: Calving fluxes and basal melt rates of Antarctic ice shelves, *Nature*, 502, 89–92, <https://doi.org/10.1038/nature12567>, 2013.
- Dinniman, Asay-Davis, X. S., Galton-Fenzi, B. K., Holland, P. R., Jenkins, A., and Timmermann, R.: Modeling ice shelf/ocean interaction in Antarctica: A review, <https://doi.org/10.5670/oceanog.2016.106>, 2016.
- Dirscherl, M., Dietz, A. J., Dech, S., and Kuenzer, C.: Remote sensing of ice motion in Antarctica – A review, *Remote Sensing of Environment*, 237, 111 595, <https://doi.org/10.1016/j.rse.2019.111595>, 2020.
- Dupont, T. and Alley, R.: Assessment of the importance of ice-shelf buttressing to ice-sheet flow., *Journal of Geophysical Research Letters*, 32, 2005.
- Fürst, J. J., Durand, G., Gillet-Chaulet, F., Tavard, L., Rankl, M., Braun, M., and Gagliardini, O.: The safety band of Antarctic ice shelves, *Nature Climate Change*, 6, 479–482, <https://doi.org/10.1038/nclimate2912>, 2016.
- Greene, C. A., Young, D. A., Gwyther, D. E., Galton-fenzi, B. K., and Blankenship, D. D.: Seasonal dynamics of Totten Ice Shelf controlled by sea ice buttressing, 12, 2869–2882, 2018.
- Gudmundsson, G.: Fortnightly variations in the flow velocity of Rutford Ice Stream, West Antarctica, *Nature*, 444, 1063–1064, <https://doi.org/10.1038/nature05430>, 2006.
- Gudmundsson, G. H.: Ice-shelf buttressing and the stability of marine ice sheets, *Cryosphere*, 7, 647–655, <https://doi.org/10.5194/tc-7-647-2013>, 2013.
- Gudmundsson, G. H., Paolo, F. S., Adusumilli, S., and Fricker, H. A.: Instantaneous Antarctic Ice Sheet mass loss driven by thinning ice shelves, *Geophysical Research Letters*, 46, 13 903–13 909, 2019.
- Gwyther, D. E., O’Kane, T. J., Galton-Fenzi, B. K., Monselesan, D. P., and Greenbaum, J. S.: Intrinsic processes drive variability in basal melting of the Totten Glacier Ice Shelf, *Nature Communications*, 9, 1–8, <https://doi.org/10.1038/s41467-018-05618-2>, 2018.
- Holland, D. and Jenkins, A.: Modeling Thermodynamic Ice–Ocean Interactions at the Base of an Ice Shelf., *Journal of Physical Oceanography*, 29, 1787–1800, <https://doi.org/10.1175/1520-0485>, 1999.
- Holland, D. M., Jacobs, S. S., and Jenkins, A.: Modelling the ocean circulation beneath the Ross Ice Shelf, *Antarctic Science*, 15, 13–23, 2003.
- Holland., P. R., Bracegirdle, T. J., Dutrieux, P., Jenkins, A., and Steig, E. J.: West Antarctic ice loss influenced by internal climate variability and anthropogenic forcing, *Nature Geoscience*, 12, 718–724, <https://doi.org/10.1038/s41561-019-0420-9>, 2019.
- Howat, I. M., Box, J. E., Ahn, Y., Herrington, A., and McFadden, E. M.: Seasonal variability in the dynamics of marine-terminating outlet glaciers in Greenland, *Journal of Glaciology*, 56, 601–613, <https://doi.org/10.3189/002214310793146232>, 2010.



- Hulbe, C., Scambos, T., Klinger, M., and Fahnestock, M.: Flow variability and ongoing margin shifts on Bindschadler and MacAyeal Ice Streams, West Antarctica, *Journal of Geophysical Research, Earth Surface*, 121, 283–293, <https://doi.org/10.1002/2015JF003670>, 2016.
- Jendersie, S., Williams, M. J. M., Langhorne, P. J., and Robertson, R.: The Density-Driven Winter Intensification of the Ross Sea Circulation, *Journal of Geophysical Research: Oceans*, 123, 7702–7724, <https://doi.org/10.1029/2018JC013965>, 2018.
- 700 Jenkins, A., Shoosmith, D., Dutrieux, P., Jacobs, S., Kim, T. W., Lee, S. H., Ha, H. K., and Stammerjohn, S.: West Antarctic Ice Sheet retreat in the Amundsen Sea driven by decadal oceanic variability, *Nature Geoscience*, 11, 733–738, <https://doi.org/10.1038/s41561-018-0207-4>, 2018.
- Joughin, Smith, B. E., and Medley, B.: Marine ice sheet collapse potentially under way for the Thwaites Glacier Basin, West Antarctica, *Science*, 344, 735–738, 2014.
- 705 Joughin, I., Alley, R. B., and Holland, D. M.: Oceanic Forcing, *Science*, 338, 1172–6, <https://doi.org/10.1126/science.1226481>, 2013.
- Joughin, I., Shapero, D., Smith, B., Dutrieux, P., and Barham, M.: Ice-shelf retreat drives recent Pine Island Glacier speedup, *Science Advances*, 7, eabg3080, 2021.
- King, M., Makinson, K., and Gudmundsson, G. H.: Nonlinear interaction between ocean tides and the Larsen C Ice Shelf system, *Geophysical Research Letters*, 38, 1–5, <https://doi.org/10.1029/2011GL046680>, 2011.
- 710 Klein, E., Mosbeux, C., Bromirski, P. D., Padman, L., Bock, Y., Springer, S. R., and Fricker, H. A.: Annual cycle in flow of Ross Ice Shelf, Antarctica: Contribution of variable basal melting, *Journal of Glaciology*, 66, 861–875, <https://doi.org/10.1017/jog.2020.61>, 2020.
- Larter, R. D.: Basal Melting, Roughness and Structural Integrity of Ice Shelves, *Geophysical Research Letters*, 49, e2021GL097421, <https://doi.org/10.1029/2021GL097421>, 2022.
- Lipscomb, W. H., Leguy, G. R., Jourdain, N. C., Asay-Davis, X., Seroussi, H., and Nowicki, S.: ISMIP6-based projections of ocean-forced Antarctic Ice Sheet evolution using the Community Ice Sheet Model, *The Cryosphere*, 15, 633–661, 2021.
- 715 Liu, H. and Miller, K.: Fracture toughness of fresh-water ice, *Journal of glaciology*, 22, 135–143, 1979.
- Losch, M.: Modeling ice shelf cavities in a z coordinate ocean general circulation model, *Journal of Geophysical Research: Oceans* (1978–2012), 113, <https://doi.org/10.1029/2007jc004368>, 2008.
- Malyarenko, A., Robinson, N. J., Williams, M. J. M., and Langhorne, P. J.: A Wedge Mechanism for Summer Surface Water Inflow Into the Ross Ice Shelf Cavity, *Journal of Geophysical Research: Oceans*, 124, 1196–1214, <https://doi.org/10.1029/2018jc014594>, 2019.
- 720 Marsh, O. J., Fricker, H. A., Siegfried, M. R., Christianson, K., Nicholls, K. W., Corr, H. F., and Catania, G.: High basal melting forming a channel at the grounding line of Ross Ice Shelf, Antarctica, *Geophysical Research Letters*, 43, 250–255, <https://doi.org/10.1002/2015GL066612>, 2016.
- Moholdt, G., Padman, L., and Fricker, H. A.: Basal mass budget of Ross and Filchner-Ronne ice shelves, Antarctica, derived from Lagrangian analysis of ICESat altimetry, *Journal of Geophysical Research: Earth Surface*, 119, 2361–2380, <https://doi.org/10.1002/2014JF003171>, 2014.
- 725 Morlighem, M., Rignot, E., Seroussi, H., Larour, E., Ben Dhia, H., and Aubry, D.: Spatial patterns of basal drag inferred using control methods from a full-Stokes and simpler models for Pine Island Glacier, West Antarctica, *Geophysical Research Letters*, 37, 1–6, <https://doi.org/10.1029/2010GL043853>, 2010.
- 730 Morlighem, M., Seroussi, H., Larour, E., and Rignot, E.: Inversion of basal friction in Antarctica using exact and incomplete adjoints of a higher-order model, *Journal of Geophysical Research: Earth Surface*, 118, 1746–1753, <https://doi.org/10.1002/jgrf.20125>, 2013.
- Mosbeux, C., Padman, L., Klein, E., Bromirski, P., and Fricker, H.: Seasonal variability in Antarctic ice shelf velocities forced by sea surface height variations, *The Cryosphere*, 17, 2585–2606, 2023.

- Mottram, R., Simonsen, S. B., Svendsen, S. H., Barletta, V. R., Sørensen, L. S., Nagler, T., Wuite, J., Groh, A., Horwath, M., Rosier, J.,  
735 Solgaard, A., Hvidberg, C. S., and Forsberg, R.: An integrated view of Greenland Ice Sheet mass changes based on models and satellite  
observations, *Remote Sensing*, 11, 1–26, <https://doi.org/10.3390/rs11121407>, 2019.
- Murray, T., Smith, A., King, M., and Weedon, G.: Ice flow modulated by tides at up to annual periods at Rutford Ice Stream, West Antarctica,  
*Geophysical Research Letters*, 34, 2007.
- Ng, F. and Conway, H.: Fast-flow signature in the stagnated Kamb Ice Stream, West Antarctica, *Geology*, 32, 481–484, 2004.
- 740 Nicolas, J. P., Vogelmann, A. M., Scott, R. C., Wilson, A. B., Cadetdu, M. P., Bromwich, D. H., Verlinde, J., Lubin, D., Russell, L. M.,  
Jenkinson, C., et al.: January 2016 extensive summer melt in West Antarctica favoured by strong El Niño, *Nature communications*, 8,  
1–10, 2017a.
- Nicolas, J. P., Vogelmann, A. M., Scott, R. C., Wilson, A. B., Cadetdu, M. P., Bromwich, D. H., Verlinde, J., Lubin, D., Russell, L. M.,  
Jenkinson, C., et al.: January 2016 extensive summer melt in West Antarctica favoured by strong El Niño, *Nature communications*, 8,  
745 15 799, 2017b.
- Padman, L., Erofeeva, S., and Joughin, I.: Tides of the Ross Sea and Ross Ice Shelf cavity, *Antarctic Science*, 15, 31–40,  
<https://doi.org/10.1017/S0954102003001032>, 2003.
- Paolo, F. S., Fricker, H. A., and Padman, L.: Volume loss from Antarctic ice shelves is accelerating, *Science*, 348, 327–331,  
<https://doi.org/10.1126/science.aaa0940>, 2015.
- 750 Pattyn, F.: Sea-level response to melting of Antarctic ice shelves on multi-centennial timescales with the fast Elementary Thermomechanical  
Ice Sheet model (f.ETISH v1.0), *Cryosphere*, 11, 1851–1878, <https://doi.org/10.5194/tc-11-1851-2017>, 2017.
- Pattyn, F. and Durand, G.: Why marine ice sheet model predictions may diverge in estimating future sea level rise, *Geophysical Research  
Letters*, 40, 4316–4320, <https://doi.org/10.1002/grl.50824>, 2013.
- Pattyn, F., Ritz, C., Hanna, E., Asay-Davis, X., DeConto, R., Durand, G., Favier, L., Fettweis, X., Goelzer, H., Golledge, N. R., Kuipers  
755 Munneke, P., Lenaerts, J. T., Nowicki, S., Payne, A. J., Robinson, A., Seroussi, H., Trusel, L. D., and van den Broeke, M.: The Greenland  
and Antarctic Ice Sheets under 1.5 °C global warming, *Nature Climate Change*, 8, 1053–1061, [https://doi.org/10.1038/s41558-018-0305-  
8](https://doi.org/10.1038/s41558-018-0305-8), 2018.
- Pawlowicz, R., Beardsley, B., and Lentz, S.: Classical tidal harmonic analysis including error estimates in MATLAB using T\_TIDE, *Com-  
puters & geosciences*, 28, 929–937, 2002.
- 760 Ranganathan, M., Minchew, B., Meyer, C. R., and Gudmundsson, G. H.: A new approach to inferring basal drag and ice rheology in ice  
streams, with applications to West Antarctic Ice Streams, *Journal of Glaciology*, 67, 229–242, <https://doi.org/10.1017/jog.2020.95>, 2021.
- Ray, R. D., Larson, K. M., and Haines, B. J.: New determinations of tides on the north-western Ross Ice Shelf., *Antarctic Science*, 33,  
89–102, <https://doi.org/10.1017/S0954102020000498>, 2021.
- Reese, R., Gudmundsson, G. H., Levermann, A., and Winkelmann, R.: The far reach of ice-shelf thinning in Antarctica, *Nature Climate  
765 Change*, 8, 53–57, <https://doi.org/10.1038/s41558-017-0020-x>, 2018.
- Retzlaff, R. and Bentley, C. R.: Timing of stagnation of Ice Stream C, West Antarctica, from short-pulse radar studies of buried surface  
crevasses, *Journal of Glaciology*, 39, 553–561, 1993.
- Rignot, Jacobs, S., Mouginot, J., and Scheuchl, B.: Ice-shelf melting around Antarctica, *Science*, 341, 266–270,  
<https://doi.org/10.1126/science.1235798>, 2013.
- 770 Rignot, Mouginot, and B. S.: MEaSURES INSAR-Based Antarctica Ice Velocity Map, Version 2, Boulder, Colorado USA. NASA National  
Snow and Ice Data Center Distributed Active Archive Center, <https://doi.org/10.5067/D7GK8F5J8M8R>, accessed on 20/02/2020, 2017.

- Rignot, E., Mouginot, J., Scheuchl, B., van den Broeke, M., van Wessem, M. J., and Morlighem, M.: Four decades of Antarctic Ice Sheet mass balance from 1979–2017, *Proceedings of the National Academy of Sciences*, 116, 1095–1103, <https://doi.org/10.1073/pnas.1812883116>, 2019.
- 775 Rosier, S. H. and Gudmundsson, G. H.: Exploring mechanisms responsible for tidal modulation in flow of the Filchner-Ronne Ice Shelf, *Cryosphere*, 14, 17–37, <https://doi.org/10.5194/tc-14-17-2020>, 2020.
- Sagebaum, M., Albring, T., and Gauger, N.: High-Performance Derivative Computations using CoDiPack, *ACM Transactions on Mathematical Software (TOMS)*, 45, <https://dl.acm.org/doi/abs/10.1145/3356900>, 2019.
- Schlegel, N. J., Seroussi, H., Schodlok, M. P., Larour, E. Y., Boening, C., Limonadi, D., Watkins, M. M., Morlighem, M., and Van Den  
780 Broeke, M. R.: Exploration of Antarctic Ice Sheet 100-year contribution to sea level rise and associated model uncertainties using the ISSM framework, *Cryosphere*, 12, 3511–3534, <https://doi.org/10.5194/tc-12-3511-2018>, 2018.
- Schodlok, M., Menemenlis, D., and Rignot, E.: Ice shelf basal melt rates around Antarctica from simulations and observations., *Journal of Geophysical Research*, 121, 1085–1109, <https://doi.org/10.1002/2015JC011117>, 2016.
- Schoof, C.: Ice sheet grounding line dynamics: Steady states, stability, and hysteresis, *Journal of Geophysical Research: Earth Surface*, 112,  
785 1–19, <https://doi.org/10.1029/2006JF000664>, 2007.
- Shepherd, A., Ivins, E. R., Geruo, A., Barletta, V. R., Bentley, M. J., Bettadpur, S., Briggs, K. H., Bromwich, D. H., Forsberg, R., Galin, N., Horwath, M., Jacobs, S., Joughin, I., King, M. A., Lenaerts, J. T., Li, J., Ligtenberg, S. R., Luckman, A., Luthcke, S. B., McMillan, M., Meister, R., Milne, G., Mouginot, J., Muir, A., Nicolas, J. P., Paden, J., Payne, A. J., Pritchard, H., Rignot, E., Rott, H., Sørensen, L. S., Scambos, T. A., Scheuchl, B., Schrama, E. J., Smith, B., Sundal, A. V., Van Angelen, J. H., Van De Berg, W. J., Van Den Broeke, M. R.,  
790 Vaughan, D. G., Velicogna, I., Wahr, J., Whitehouse, P. L., Wingham, D. J., Yi, D., Young, D., and Zwally, H. J.: A reconciled estimate of ice-sheet mass balance, *Science*, 338, 1183–1189, <https://doi.org/10.1126/science.1228102>, 2012.
- Shepherd, A., Fricker, H. A., and Farrell, S. L.: Trends and connections across the Antarctic cryosphere, *Nature*, 558, 223–232, <https://doi.org/10.1038/s41586-018-0171-6>, 2018.
- Stern, A. A., Dinniman, M. S., Zagorodnov, V., Tyler, S. W., and Holland, D. M.: Intrusion of warm surface water beneath the McMurdo ice shelf, Antarctica, *Journal of Geophysical Research: Oceans*, 118, 7036–7048, <https://doi.org/10.1002/2013JC008842>, 2013.
- 795 Stevens, C., Hulbe, C., Brewer, M., Stewart, C., Robinson, N., Ohneiser, C., and Jendersie, S.: Ocean mixing and heat transport processes observed under the Ross Ice Shelf control its basal melting, *Proceedings of the National Academy of Sciences of the United States of America*, 117, 16 799–16 804, <https://doi.org/10.1073/pnas.1910760117>, 2020.
- Stevens, L. A., Nettles, M., Davis, J. L., Creyts, T. T., Kingslake, J., Ahlstrøm, A. P., and Larsen, T. B.: Helheim Glacier diurnal velocity  
800 fluctuations driven by surface melt forcing, *Journal of Glaciology*, 68, 77–89, <https://doi.org/10.1017/jog.2021.74>, 2022.
- Stewart, C. L., Christoffersen, P., Nicholls, K. W., Williams, M. J., and Dowdeswell, J. A.: Basal melting of Ross Ice Shelf from solar heat absorption in an ice-front polynya, *Nature Geoscience*, 12, 435–440, <https://doi.org/10.1038/s41561-019-0356-0>, 2019.
- Still, H., Campbell, A., and Hulbe, C.: Mechanical analysis of pinning points in the Ross Ice Shelf, Antarctica, *Annals of Glaciology*, 60, 32–41, <https://doi.org/10.1017/aog.2018.31>, 2019.
- 805 Tétéault, P., Kouba, J., Héroux, P., and Legree, P.: CSRS-PPP: an internet service for GPS user access to the Canadian Spatial Reference Frame, *Geomatica*, 59, 17–28, 2005.
- Thomas, R., Scheuchl, B., Frederick, E., Harpold, R., Martin, C., and Rignot, E.: Continued slowing of the Ross Ice Shelf and thickening of West Antarctic ice streams, *Journal of Glaciology*, 59, 838–844, <https://doi.org/10.3189/2013JoG12J122>, 2013.

- Tinto, K. J., Padman, L., Siddoway, C. S., Springer, S. R., Fricker, H. A., Das, I., Caratori Tontini, F., Porter, D. F., Frearson, N. P., Howard, S. L., Siegfried, M. R., Mosbeux, C., Becker, M. K., Bertinato, C., Boghosian, A., Brady, N., Burton, B. L., Chu, W., Cordero, S. I., Dhakal, T., Dong, L., Gustafson, C. D., Keeshin, S., Locke, C., Lockett, A., O'Brien, G., Spergel, J. J., Starke, S. E., Tankersley, M., Wearing, M. G., and Bell, R. E.: Ross Ice Shelf response to climate driven by the tectonic imprint on seafloor bathymetry, *Nature Geoscience*, 12, 441–449, <https://doi.org/10.1038/s41561-019-0370-2>, 2019.
- Trusel, L., Frey, K., Das, S., Karnauskas, K., Munneke, P., Meijgaard, E., and Van den Broeke, M.: Divergent trajectories of Antarctic surface melt under two twenty-first-century climate scenarios, *Nature Geoscience*, 8, 927–932, <https://doi.org/10.1038/ngeo2563>, 2015.
- van der Wel, N., Christoffersen, P., and Bougamont, M.: The influence of subglacial hydrology on the flow of Kamb Ice Stream, West Antarctica, *Journal of Geophysical Research: Earth Surface*, 118, 97–110, 2013.
- Van Wessem, J. M., van de Berg, W. J., Noël, B. P. Y., van Meijgaard, E., Amory, C., Birnbaum, G., Jakobs, C. L., Krüger, K., Lenaerts, J. T. M., Lhermitte, S., Ligtenberg, S. R. M., Medley, B., Reijmer, C. H., van Tricht, K., Trusel, L. D., van Uft, L. H., Wouters, B., Wuite, J., and van den Broeke, M. R.: Modelling the climate and surface mass balance of polar ice sheets using RACMO2 – Part 2: Antarctica (1979–2016), *The Cryosphere*, 12, 1479–1498, <https://doi.org/10.5194/tc-12-1479-2018>, 2018.
- Vaughan, D. G. and Doake, C.: Recent atmospheric warming and retreat of ice shelves on the Antarctic Peninsula, *Nature*, 379, 328–331, 1996.
- Whiteford, A., Horgan, H., Leong, W., and Forbes, M.: Melting and refreezing in an ice shelf basal channel at the grounding line of the Kamb Ice Stream, West Antarctica, *Journal of Geophysical Research: Earth Surface*, 127, e2021JF006 532, 2022.
- Zou, X., Bromwich, D. H., Montenegro, A., Wang, S.-H., and Bai, L.: Major surface melting over the Ross Ice Shelf part I: Foehn effect, *Quarterly Journal of the Royal Meteorological Society*, 147, 2874–2894, 2021a.
- Zou, X., Bromwich, D. H., Montenegro, A., Wang, S.-H., and Bai, L.: Major surface melting over the Ross Ice Shelf part II: Surface energy balance, *Quarterly Journal of the Royal Meteorological Society*, 147, 2895–2916, 2021b.
- Zumberge, J., Heflin, M., Jefferson, D., Watkins, M., and Webb, F.: Precise point positioning for the efficient and robust analysis of GPS data from large networks, *Journal of geophysical research: solid earth*, 102, 5005–5017, 1997.